NEURONAL ACTIVITY DRIVES LOCALIZED BLOOD-BRAIN-BARRIER TRANSPORT OF SERUM INSULIN-LIKE GROWTH FACTOR-I INTO THE CENTRAL NERVOUS SYSTEM

[1]T. Nishijima*, [1]J. Piriz*[Θ], [1]S. Duflot*, [1]A.M. Fernandez, [1]G. Gaitan, [2]U. Gomez-Pinedo, [2]J.M. Verdugo, [1]F. Leroy, [3]H. Soya, [4]A. Nuñez, and [1]I. Torres-Aleman

[1]Cajal Institute, CSIC and CIBERNED, Madrid, Spain. [2]University of Valencia, CIPF, and CIBERNED, Valencia; Spain. [3]University of Tsukuba, Tsukuba, Japan. [4]Autonoma University, Madrid, Spain.

Correspondence to Ignacio Torres Aleman. Cajal Institute. Avda Dr Arce 37, Madrid 28002. Spain

Running title: Activity-dependent entrance of serum IGF-I

* These authors contributed equally to this work. [Θ] Present address: Laboratorio de Fisiologia y Biologia Molecular (LFBM-IFIBYNE). Buenos Aires, Argentina.

Summary

Upon entry into the central nervous system (CNS), serum insulin-like growth factor-1 (IGF-I) modulates neuronal growth, survival and excitability. Yet mechanisms that trigger IGF-I entry across the blood-brain barrier remain unclear. We show that neuronal activity elicited by electrical, sensory or behavioral stimulation increases IGF-I input in activated regions. Entrance of serum IGF-I is triggered by diffusible messengers (i.e. ATP, arachidonic acid derivatives) released during neuro-vascular coupling. These messengers stimulate matrix metalloproteinase-9, leading to cleavage of the IGF binding protein-3

(IGFBP-3). Cleavage of IGFBP-3 allows the passage of serum IGF-I into the CNS through an interaction with the endothelial transporter lipoprotein related receptor 1. Activity-dependent entrance of serum IGF-I into the CNS may help to explain disparate observations such as pro-neurogenic effects of epilepsy, rehabilitatory effects of neural stimulation and modulatory effects of blood flow on brain activity.

Introduction

The blood-brain-barriers (BBB) located at brain vessels and choroid plexuses regulate passage of blood constituents into the brain parenchyma and cerebrospinal fluid (CSF), respectively (Abbott et al., 2010). Once considered an almost impermeable barrier for serum proteins, it is now apparent that many circulating hormones and growth factors can cross the BBB through specific transport mechanisms that usually involve their cognate receptors (Banks, 2006). However, the physiological significance of this blood-to-brain traffic of hormones and growth factors remains uncertain.

Insulin-like growth factor I (IGF-I), a peptide with ample neuroprotective activity (Russo et al., 2005), is one of the growth factors found to enter the brain from the circulation (Pardridge, 1993; Carro et al., 2000; Pulford and Ishii, 2001; Reinhardt and Bondy, 1994). Circulating IGF-I is produced mostly by the liver and is an important mediator of growth hormone actions in body growth and tissue remodelling . In addition, serum IGF-I shows a wide neuroactive profile that hints to an important role in brain homeostasis. Thus, blood-borne IGF-I modulates brain vessel growth (Lopez-Lopez et al., 2004), adult neurogenesis (Aberg et al., 2000), neuronal excitability (Nunez et al., 2003), or even cognitive function (Trejo et al., 2007). Collectively these observations provide a strong rationale for the need of circulating IGF-I to cross the BBB. Notably, the BBB

architecture is well suited to transport serum IGF-I into the brain as both brain vessels and glial end-feet surrounding them express IGF-I receptors (Garcia-Segura et al., 1991). If IGF-I is transferred by endothelial cells into the perivascular space, surrounding glial end-feet from astrocytes, able to endocytose IGF-I (Auletta et al., 1992), could transfer IGF-I to adjacent neurons through trans-endocytosis or a related process. Indeed, while upon binding to its membrane receptor IGF-I is internalized and mostly degraded (Geary et al., 1989), several cell types can translocate intact IGF-I to other cell compartments or even export it outside the cell (Zapf et al., 1994).

The choroid plexus epithelium at the blood-CSF interface also express high levels of IGF-I receptors (Marks et al., 1991). In previous work we found that increases in systemic IGF-I led to increased passage into the CSF through a mechanism involving the multicargo protein transporter low density lipoprotein receptor related protein 2 (LRP2) located in this sealed epithelium (Carro et al., 2000;Carro et al., 2005). Therefore, a tonic transfer of serum IGF-I into the CSF may be explained by physiological oscillations in blood IGF-I levels (Carro et al., 2000). However, serum IGF-I levels usually remain very steady. Thus, a mechanism involving regulated passage of serum IGF-I may also co-exist with this tonic input. A possible regulatory mechanism independent of changes in serum IGF-I levels may be activity-driven.

Brain activity dictates transfer of oxygen and nutrients from the circulation into activated regions through a “neuro-vascular coupling” process described long ago (Roy and Sherrington, 1890). This process recruits all the cellular components of the neuro-vascular unit, with astrocytes serving an important intermediary role between neuronal activation and endothelial transport of oxygen and glucose (Zonta et al., 2003). While the intracellular pathways involved in neuro-vascular coupling are not fully understood, a wealth of data

indicate that diverse mediators released in response to neuronal glutamate (arachidonic acid derivatives, ATP...etc) influence the microcirculation allowing local increased passage of glucose and other nutrients through brain endothelial cells.

IGF-I in blood travels as a complex with an insulin-like binding protein 3 (IGFBP-3) and an "acid labile subunit" chaperone that regulates availability to target tissues by regulated release of IGF-I. Although the details of the trans-endothelial transport of IGF-I are not known, the tertiary complex probably tethers/associates to blood vessels to deliver IGF-I to endothelial cells after cleavage of IGFBP-3 by proteases. IGFBP-3 associates to the extracellular matrix and to membrane proteins such as LRP1. This membrane cargo-transporter mediates transcytosis of ligands across brain endothelial cells and has been postulated to be a cellular receptor for IGFBP-3 (Huang et al., 2003). LRP1 is abundantly expressed in brain endothelium and interacts with the insulin receptor (Bilodeau et al., 2009), which is closely related to the IGF-I receptor. Altogether, these characteristics make LRP-1 an attractive candidate to serve as a targeting platform for the circulating IGF-I/IGFBP-3 complex.

In the present work we explored whether brain activity modulates entrance of serum IGF-I and possible mechanisms involved. We observed that serum IGF-I input to the brain is regulated by an activity-driven process that includes changes in BBB permeability to serum IGF-I. This process is initiated by the release of glutamate at active regions. Thereafter, two parallel processes are set in motion; vasodilation to increase local availability of serum IGF-I, and increased activity of matrix metalloprotease 9 (MMP9), an IGFBP3 protease already reported to be released in response to neuronal activity (Michaluk and Kaczmarek, 2007). The combined action of these two processes result in increased

local availability of free serum IGF-I that is transcytosed through an LRP1-dependent mechanism.

Results

Neuronal activity stimulates uptake of serum IGF-I.

To assess mechanisms by which IGF-I might penetrate the BBB in response to neuronal activity we used a combination of experimental approaches. First, we placed a stimulating electrode in the inferior cerebellar peduncle of rats receiving a bolus injection of human recombinant IGF-I (hIGF-I; 10µg/100g) in the carotid artery immediately before stimulation. Using a human-specific IGF-I ELISA we distinguished between exogenous and endogenous (rat brain) IGF-I. As previously documented (Carro et al., 2000), hIGF-I was detected in different brain regions after systemic delivery. However, electrical stimulation (15 min, 5 Hz) of the cerebellar peduncle elicited an additional significant increase in cerebellar hIGF-I levels (Figure 1A). Non-stimulated regions such as the cerebral cortex did not show differences between stimulated and sham-stimulated animals (Figure 1A).

To assess whether systemic IGF-I accumulates in active brain areas regardless of region and type of stimulus, we activated the rat somatosensory cortex by unilateral whisker stimulation (60 min, 2 or 5 Hz). As seen in Figure 1B, stimulation of the vibrissae at 2 Hz effectively activated cortical somatosensory neurons, whereas at 5 Hz stimulation was dumped (inset) due to neuronal desensitization (Chung et al., 2002). Accordingly, only stimulation of the whiskers at 2 Hz increased hIGF-I in somatosensory cortex as compared to animals stimulated at 5 Hz, or sham-stimulated animals (Figure 1B). Frequency-dependence uptake of IGF-I by the brain correlates with frequency-dependent changes in

cerebral blood flow in the barrel cortex during whisker stimulation (see below). These observations further confirmed that entrance of systemic IGF-I is regulated by neuronal activity. A region unrelated to the stimulation site such as the olfactory bulb, that had relatively high levels of hIGF-I after systemic injection, did not show stimulus-dependent increases in hIGF-I (not shown). Local IGF-I synthesis was not modified by stimulation; IGF-I mRNA levels in the stimulated somatosensory cortex did not differ from those in the unstimulated side (Fig S1A). Further, the IGF-I receptor was more activated in the stimulated than in the non-stimulated somatosensory cortex, as determined by increased levels of the Tyr-phosphorylated form of the receptor (Figure 1C). The latter confirms increased IGF-I input in the stimulated area.

We next assessed whether natural alterations in brain activity patterns, resulting from normal behavioral patterns, regulate IGF-I entry into the CNS. Mice submitted to a brief episode (2 hours) of environmental enrichment including multiple sensori-motor stimuli and increased social engagement showed a 60% increase in hippocampal IGF-I levels compared to animals staying in their normal cages (Figure 1D). In addition, phosphorylation levels of hippocampal IGF-I receptor were significantly higher after environmental enrichment (Figure 1E). Thus, IGF-I input to this brain area appears augmented by environmental enrichment.

As systemic administration of IGF-I modulates basal neuronal excitability (Nunez et al., 2003), we determined whether IGF-I also influences neuronal output in stimulated brain areas. Infusion of the IGF-I receptor antagonist PPP in the somatosensory cortex during unilateral tactile stimulation of the whiskers significantly reduced neuronal activation in this area. Under control conditions, whisker deflections (20 ms duration) induced spike firing in the primary somatosensory cortex of 2.9 spikes/stimulus (Figure 1F). However,

intracortical application of PPP (2.5 μM) reduced cortical responses to 2.2 spikes/stimulus 15 min after application ($p=0.005$), and to 1.9 spikes/stimulus 30 min later (Figure 1F, lower panel; n= 19 cells; $p=0.004$). These results strongly suggest that IGF-I input into active brain regions has a functional impact.

Activity-dependent entrance of serum IGF-I across brain vessels.

Albeit at lower levels, non-stimulated brain areas also accumulate hIGF-I after intracarotid injection (i.e.: cortex in Figure 1A). Hence, we next determined whether systemic hIGF-I entered into the brain after neuronal activation through the blood-CSF interface (Carro et al., 2000). We assessed levels of hIGF-I in CSF after whisker stimulation and found no changes as compared to non-stimulated animals (Fig S1B). This suggested that activity-dependent entrance of systemic hIGF-I occurs through a different pathway. In agreement with this, when hIGF-I (5 μg/rat) was directly delivered into the CSF (Fig S1C), no stimulus-dependent increases of hIGF-I in the activated somatosensory cortex were seen (Fig S1D). This also indicated that cerebrospinal fluid IGF-I does not redistribute to active brain regions. Hence, the other possible route of entrance of circulating IGF-I into active brain areas is the local vasculature. Indeed, administration of digoxigenin-labelled IGF-I (Dig-IGF-I) immediately before stimulation of the whiskers or the sciatic nerve resulted in specific digoxigenin immunostaining in the stimulated side of the somatosensory cortex (Figure 2A). Double immunostaining with cell-specific markers showed that Dig-IGF-I staining colocalized with brain vessels (lectin$^+$ cells), astrocytes (GFAP$^+$), and neurons ($\beta_3$tubulin$^+$) (Figure 2B). Cells with neuronal morphology co-stained for digoxigenin and IGF-I, indicating that digoxigenin remained attached to IGF-I (Fig S2A). Non-stimulated animals did not show immunoreactivity in somatosensory cortex (Figure 2A, panel b). Further, Dig-IGF-I staining was also prominent in the posterio-medial

thalamus (Figure 2C) contralateral to the stimulated whisker pad. As this thalamic relay is within the whisker-cortex pathway this suggests an spatial overlap between activated areas and IGF-I uptake. In this regard, neuronal activation determined by c-fos immunoreactivity showed overlapping of Dig-IGF-I staining with active brain regions within this sensory pathway such as the sensitive nucleus of the trigeminal nerve, the lateral thalamus and the primary somatosensory cortex (Figure 2D). Electron microscopy analysis combined with immunogold labelling confirmed the presence of Dig-IGF-I in various cell compartments of brain vessels and neurons (Figure 3). Staining was observed in the cell nucleus, mitochondria and cytoplasm.

Neuro-trophic coupling through activity-dependent mediators.

We next searched for mechanisms underlying activity-dependent entrance of systemic IGF-I through the brain vasculature. We focused on neuro-vascular coupling as it involves activity-dependent signalling from active synapses that modulate neighbouring blood vessels to enhance local blood flow. As expected, unilateral electrical stimulation of the whisker pad enhanced regional cerebral blood flow (CBF) in the activated somatosensory cortex (Figure 4A). Increases in CBF were frequency-dependent. Whereas stimulation at 2 Hz consistently raised it, at 5 Hz only a transient increase was observed (Figure S3A). This observation linked neuronal blood flow with IGF-I entrance as at 5Hz no increases in hIGF-I entrance were appreciated (Figure 1B). Blood pressure, body temperature and other systemic parameters (PCO_2, PO_2..etc) remained stable during stimulation of the animals (Table 1). No changes were observed in CBF at the unstimulated barrel cortex (not shown). As IGF-I may act as a vasodilator, we determined whether intracarotid administration of IGF-I alters CBF in somatosensory cortex of non stimulated animals, and found no changes (Fig S3B).

Confirming the above observations, hIGF-I levels were significantly elevated in brain interstitial fluid collected through a microdialysis probe placed in the somatosensory cortex of animals receiving vibrissae stimulation at 2 Hz ($p<0.01$; Figure 4B). Using this approach we determined the role of neuronal activity and vasodilation in activity-dependent IGF-I uptake. Intra-cortical infusion of TTX to inhibit neuronal activity (markedly reducing stimulus-induced increases in CBF, see Figure S3C), abrogated the increase in hIGF-I levels induced by vibrissae stimulation (Figure 4B). Similarly, infusion of the NO synthase inhibitor L-NAME to block vasodilation (that also results in diminished CBF after whisker stimulation, see Fig S3C), also abrogated this increase (Figure 4B). Collectively, these results indicate that both enhanced neuronal activity and increased blood flow are necessary for activity-dependent increases in serum IGF-I input to the brain.

As passage of serum IGF-I through blood-brain-barrier cells may involve all the cells forming the neurovascular unit, we then used an *in vitro* system to determine whether the three main types of cells potentially involved in this purported blood-to-brain trafficking of IGF-I can internalize it. We found that endothelial cells, astrocytes, and neurons internalize intact biotinylated hIGF-I (bhIGF-I) after adding it to the culture medium (Figure 5A, upper blot). Elimination of non-specific protein binding to the cell membrane prior to cell lysis by acid wash confirmed that the 3 types of cells internalize bhIGF-I (Figure 5A, lower blots). Further, as shown in Figure 5A, double immunostaining of biotin-labelled IGF-I and cell-specific markers show bhIGF-I immunoreactivity in endothelial cells (lectin$^+$ cells), astrocytes (GFAP$^+$), and neurons ($\beta_3$tubulin$^+$). We then hypothesized that once IGF-I binds to its receptors in endothelial cells, it will be internalized and translocated to adjacent glial end-feet surrounding brain vessels through a transcytosis process. To analyze this point we used a double chamber culture system with astrocytes as a feeder layer of endothelial cells

in the upper chamber, and neurons placed in the lower chamber to mimic the BBB architecture. Under these conditions bhIGF-I was transported from the upper (i.e.: apical side or "blood side"of the endothelial monolayer) to the lower chamber (basolateral side or "brain side") where neurons accumulated it (Figure 5B).

Next, we determined whether IGFBP-3 modulates internalization of IGF-I by endothelial cells. In the presence of IGFBP-3 (15 ng/ml) a weak, but significant decrease in bhIGF-I endocytosis by brain endothelial cell cultures was observed (Figure 5C). The modest effect of exogenous IGFBP-3 could be due to the presence of endogenous IGFBP-3, as endothelial cells produce this binding protein (Lee et al., 1999). Indeed, IGFBP-3 was detected in the cultures (Figure 5D). To further substantiate a role of this binding protein in internalization of IGF-I by brain endothelial cells we determined whether prostate specific antigen (PSA), an IGFBP-3 protease, affected internalization of bhIGF-I. Addition of PSA greatly increased internalization of bhIGF-I by endothelial cells (Figure 5C). As the effect was antagonized by IGFBP-3 (Figure 5C) this further supports its involvement. Further, endocytosis of bhIGF-I required the IGF-I receptor. Either transfection of human endothelioma cells with a dominant-negative IGF-I receptor (Figure 5E) or incubation of brain endothelial cells with the IGF-I receptor antagonist PPP blocked IGF-I internalization (Figure S4A).

Because PSA is a prostate protease unlikely to be produced by brain cells, we searched for alternative protease(s) involved in IGFBP-3 cleavage in brain endothelium. Among potential candidates we chose matrix metalloproteinase-9 (MMP9). MMP9 not only cleaves this binding protein (Manes et al., 1999) (Figure 5F), but is present in brain endothelium (Wang et al., 2006), and, most significantly, is modulated by brain activity (Michaluk and Kaczmarek, 2007). In the presence of active, but not inactive MMP9 (50 ng/ml), brain

endothelial cells endocytosed significantly more bhIGF-I. The effect was inhibited by IGFBP-3 ($p<0.001$; Figure 5C). In contrast, another metalloprotease such as MMP8 did not increase IGF-I internalization by endothelial cells (Figure S4B). That another IGFBP-3 protease increased basal endocytosis confirmed that endothelial IGFBP-3 is interfering with bhIGF-I endocytosis in our cultures.

To gain further insight into the mechanism underlying transcytosis of IGF-I we used the double chamber system mimicking the BBB, omitting neurons in the lower chamber to avoid IGF-I uptake. Under these conditions bhIGF-I was transported from the upper (i.e.: apical side or "blood side"of the endothelial monolayer) to the lower chamber (basolateral side or "brain side"), and its transport was significantly reduced when IGFBP-3 was added to the upper chamber ($p<0.05$; Figure 6A). Confirming the effects seen in endothelial cell cultures, MMP9 also induced transcytosis of bhIGF-I through endothelial-astrocyte co-cultures, an effect blocked by IGFBP-3 ($p<0.01$; Figure 6A).

A key aspect of our proposal is that neuronal activation triggers serum IGF-I transcytosis from the blood into the brain. Glutamate released during neuronal activation signals to surrounding astrocytes (Haydon and Carmignoto, 2006;Perea et al., 2009) that in turn release vasoactive mediators (Iadecola and Nedergaard, 2007;Zonta et al., 2003). Accordingly, when glutamate (100 μM) was placed in the lower chamber (the brain side) of endothelial-astrocyte co-cultures, IGF-I transcytosis from the upper (the blood side) to the lower chamber was greatly stimulated ($p<0.01$; Figure 6B). The stimulatory action of glutamate was fully abolished by an MMP9 inhibitor, reinforcing a role for this protease in transcytosis of IGF-I (Figure 6B). Moreover, MMP9 was readily detected in endothelial cells (Figure 6C, upper blots) and glutamate stimulated it in endothelial-astrocyte co-cultures (Figure 6C). In agreement with this, and as expected for a protease that is

stimulated by brain activity (Michaluk and Kaczmarek, 2007), active MMP9 was increased in the stimulated somatosensory cortex (Figure 6D).

Next, we tested various vasoactive mediators proposed to be released in response to glutamate (Iadecola and Nedergaard, 2007). Among these, we chose those previously reported to enhance MMPs activity. The arachidonic acid derivatives prostaglandin E_2 (PGE_2) and 11,12 epoxyeicosatrienoic acid (EET), together with ATP, but not NO, increased bhIGF-I endocytosis by endothelial cells (Figure 7A). Another EET derivative, 8,9 EET, with lower vasodilatory activity (Harder et al., 1998) elicited a slightly smaller response: 70 ± 13% of the that seen with 11,12 EET. Confirming these in vitro observations, infusion of a pharmacological dose of PGE_2 (5 mM) into the rat cerebral cortex (-0.5 mm from bregma, 1 mm depth) elicited widespread uptake of systemic digoxigenin-labelled IGF-I in the infused side (Figure 7B). Moreover, levels of PGE_2 in stimulated somatosensory cortex increased to 4.2 ± 0.01 pg/ml from 1.9 ± 0.01 pg/ml seen in sham-stimulated cortex ($p<0.01$, n=5 per group). While these levels are well below the pharmacological doses used by us they reinforce that local increases in PGE_2 participate in serum IGF-I transfer to the brain. We then determined whether these mediators require MMP-9 to increase IGF-I transcytosis. In the presence of an MMP9 inhibitor (inhMMP9), *in vitro* transcytosis of bhIGF-I by ATP, PGE_2, or EET was abrogated (Figure 7C). As in the case of PGE_2 this inhibition was not as complete as with the other mediators, it is possible that PGE_2 recruits additional IGFBP-3 proteases.

Thereafter, we confirmed that MMP9 participates in activity-dependent uptake of serum IGF-I by the brain *in vivo*. Infusion of inhMMP9 into the somatosensory cortex of whisker-stimulated rats blocked the increase in brain interstitial fluid hIGF-I elicited by vibrissae stimulation (Figure 4B). Non-specific hemodynamic responses of inhMMP9 were ruled out

by infusing it into the somatosensory cortex and determining CBF responses to whisker stimulation (Fig S3C).

We next conducted an initial characterization of intracellular pathways involved in transfer of IGF-I in response to glutamate. We found that addition of a Ca^{++} chelator (EGTA) to the culture medium inhibited the stimulatory action of glutamate on IGF-I transcytosis through astrocyte-endothelial cells co-cultures, suggesting that the process is calcium-dependent (Table 2). Co-addition of thapsigargin, an inhibitor of the ryanodine receptor that blocks intracellular Ca^{++} stores also resulted in abrogation of IGF-I transfer, further indicating the involvement of Ca^{++} fluxes in this process (Table 2). Next, we tested various glutamate receptors antagonists and found that inhibition of ionotropic AMPA/Kainate receptors with CNQX or of mGluR5 with MPEP abrogated glutamate actions whereas NMDA and mGluR1 antagonists (AP5 and Lyly, respectively) did not alter the effect of glutamate (Table 2). Further, inhibition of prostanoid synthesis with the Cox inhibitor ibuprofen similarly blocked glutamate effects. Finally, no effect on glutamate actions was seen after inhibition of purinergic signalling using suramin (Table 2). Altogether, these results indicate that non-NMDA ionotropic and GluR5 metabotropic glutamate receptors are involved in transfer of IGF-I through astrocyte/endothelial co-cultures and that prostanoid synthesis is required for this effect.

In response to neuronal activation local levels of circulating IGF-I/IGFBP3 will increase as a result of increased local blood flow. We postulated that this complex would interact with LRP1/IGF-IR at endothelial cells for subsequent transcytosis of IGF-I. Confirming observations by others (Huang et al., 2003), we observed that LRP1 interacts with IGFBP3. LRP1 was co-immunoprecipitated with IGFBP3 in cell extracts from endothelial cultures treated with IGFBP3 (Figure 8A). LRP1 also co-immunoprecipitated with the IGF-I

receptor in brain endothelial cells (Figure 8B). Conversely, an HA-tagged mini-LRP1 (lacking most of the extracellular domain of LRP1) expressed in brain endothelial cells co-immunoprecipitated with IGF-IR (Figure 8C). This suggested that the interaction between LRP1 and IGF-IR does not involve the extracellular ligand-binding domain of LRP1, leaving this domain free for binding of extracellular ligands such as IGFBP3. Finally, while endothelial cells expressing mini-LRP-1 internalized significantly more bhIGF-I than control cells (Figure 8D), HCMEC-D3 endothelioma cells expressing LRP1 siRNA internalized markedly less bhIGF-I than scramble siRNA-transfected cells (Figure 8E, F). Thus, interaction of LRP-1 with the IGF-I receptor and IGFBP-3 may target the IGF-I/IGFBP-3 complex to the IGF-I receptor and facilitate the subsequent transcytosis of IGF-I.

Discussion

The present results indicate that brain activity drives serum IGF-I input to activated areas. This novel link between neuronal activation and localized trophic support appears to recruit processes also involved in neuro-vascular coupling (Figure 8G). The fact that similar processes participate in allocating nutrient/oxygen supply and at the same time trophic support to active brain regions widens the physiological significance of activity-dependent processes in the brain. Importantly, these observations also provide a regulatory mechanism for the neuroactive actions of blood-borne IGF-I.

In line with these observations, the increases previously observed in the number of IGF-I immunoreactive neurons in the developing rat visual cortex after experience-dependent neuronal activity (Ciucci et al., 2007), or after environmental enrichment (Guzzetta et al., 2009) may be explained by localized transfer of serum IGF-I to the brain. Also, higher brain activity observed in human subjects with higher serum IGF-I levels (Arwert et al.,

2005) agree with these findings. Together with recent evidence that neuronal activity increases anti-oxidant defences in neurons (Leveille et al., 2010;Papadia et al., 2008), these data provide further insight into the neuroprotective effects of neuronal activity.

Transcytosis of molecules across the BBB is the most common way to modulate the permeability of this barrier (Banks, 2010). Neuronal activity modulates BBB permeability through neurovascular coupling. In turn, serum IGF-I participates in brain processes where neuronal activity is involved (synaptic plasticity, cognition...etc). Therefore, we reasoned that neuronal activity could influence BBB permeability to serum IGF-I. While activity-driven neuro-vascular and neuro-trophic coupling may share common upstream mechanisms such as vasodilation (Figure 8G), downstream mechanisms leading to increase glucose uptake and IGF-I transfer respectively, probably diverge. In the former case neuronal release of glutamate leads to Ca^{++} fluxes in astrocytes and subsequent release of diffusible mediators such as NO, arachidonic acid derivatives, ATP...etc that modulate the microcirculation. Eventually, glucose and oxygen uptake are locally enhanced. Glucose uptake through the BBB is increased because glucose transporters are translocated to the cell membrane in response to a signalling mechanism that is still not well characterized. In neuro-trophic coupling, our initial observations suggest that together with vasodilation that will increase local availability of circulating IGF-I, glutamate release activates MMP9 in a process that appears to recruit several, but not all of the mediators involved in vasogenic aspects of neurovascular coupling and that also involves Ca^{++} mobilization. Thus, our initial in vitro pharmacological characterization suggest that IGF-I transfer depends on ionotropic (AMPA/kainate) and metabotropic (mGluR5) glutamate receptors, arachidonic acid derivatives and Ca^{++} fluxes. However, more work is needed to ascertain the cellular and molecular pathways involved. In this regard, it should be noted that after many years of

study, the mechanisms underlying neuro-vascular coupling are still under intense scrutiny (Shi et al., 2008).

At any rate, the present results allow us to propose an overview of the possible processes involved. Besides local changes in blood flow (in vivo inhibition of NO blocks IGF-I transfer), activation of MMP9 (and other proteases?) by diverse mediators (prostanoids, EETs, ATP) appears as the distinct characteristic required in IGF-I transfer across the BBB. MMP9 links neuronal activation with transfer of blood-borne IGF-I through an LRP1-dependent process. A similar process probably takes place at the choroid plexus, where the closely related receptor LRP2 also binds to the IGF-I receptor and actively participates in IGF-I transcytosis (Carro et al., 2005). Thus, two parallel processes, neuro-vascular coupling, and neuro-trophic coupling, are set in motion by glutamate release at active synapses.

Several questions remain open. For instance, while the absence of changes in IGF-I mRNA synthesis after brain activation suggests that brain activity does not induce local IGF-I synthesis, locally activated IGF-I protein translation cannot be ruled out. This possibility would require further study. Further, while IGF-I immunoreactivity in the nucleus of astrocytes and neurons was already observed by us (Garcia-Segura et al., 1991), and more recently confirmed in other cell types (Sehat et al., 2010), the role that IGF-I may play in these cellular organelles is still not fully understood.

Our observations also provide a mechanistic support for the cognitive reserve hypothesis of neuroprotection. Conceivably, neuro-trophic coupling may contribute to the beneficial effects of an active social life and higher education on brain function (Fratiglioni et al., 2004). As neuroprotective behaviors such as exercise or balanced diets also favor entrance of serum IGF-I into the brain (Carro et al., 2000;Dietrich et al., 2007) this neuroprotective

serum growth factor may be considered a common mediator of the beneficial effects of diverse life-style factors on brain health.

These findings may help explain disparate observations such as the pro-neurogenic effect of epilepsy or electroconvulsive therapy (Kempermann, 2002), the modulatory effect of blood flow on neuronal activity (Moore and Cao, 2007), or the rehabilitatory effect of neural stimulation (Kaelin-Lang, 2008). The latter may be of particular practical impact. The unifying thread in all these processes would be increased input of serum IGF-I to stimulated brain regions. In the first case enhanced neurogenesis after neuronal hyper-activity could be explained by the potent neurogenic effects documented for serum IGF-I (Trejo et al., 2008). In the second case, activity-dependent entrance of serum IGF-I coupled to enhanced blood flow would conform to the "hemo-neural" hypothesis that proposes that diffusible blood-borne messengers modulate neuronal activity (Moore and Cao, 2007). Indeed, systemic IGF-I increases neuronal excitability (Nunez et al., 2003) and levels of serum IGF-I correlate with brain vascular activation (Arwert et al., 2005). Finally, neural stimulation inducing the entrance of systemic IGF-I will in turn produce wide beneficial effects on activated areas through the ample neuroprotective actions of IGF-I (Carro et al., 2003). An unexplored aspect of these observations is the angiogenic role of serum IGF-I (Lopez-Lopez et al., 2004). As vessel formation is regulated by tissue demand, activity-dependent uptake of serum IGF-I through brain vessels would also impinge on vessels themselves. Altogether, activity-dependent entrance of a serum neuroprotective factor supports the use of neuro-rehabilitation procedures based on targeted neuronal stimulation of damaged areas.

LEGENDS TO FIGURES

Figure 1: Active brain areas accumulate systemic IGF-I. **A,** Electrical stimulation of the rat cerebellar peduncle (black bars) increased hIGF-I levels in cerebellum, as compared to sham-stimulated rats (white bars). Unstimulated areas such as the cerebral cortex did not show differences between stimulated and non-stimulated animals. Rats received hIGF-I through the carotid artery before stimulation of the inferior cerebellar peduncle (n=7 per group; *p<0.05). **B,** Electrical stimulation of the rat whiskers increased hIGF-I in the contralateral somatosensory cortex in a frequency-dependent fashion. Unilateral vibrissae stimulation at 2 Hz activates cortical somatosensory neurons, whereas at 5 Hz stimulation is dumped due to neuronal desensitization (inset shows averages of representative vibrissae deflection responses at somatosensory cortex; n=10; *p<0.05). Sham: non-stimulated animals. **C,** In 2 Hz-stimulated animals, levels of pTyr IGF-IR were significantly higher in the stimulated barrel cortex than in the ipsilateral, non-stimulated side (n=10, **p<0.01). Four representative animals (coded 1-4) are shown in blot. Quantitation histograms are shown after normalization with total IGF-IR levels (lower blot). Con: control, non-stimulated side, St, stimulated side. IgGs: band corresponding to the antibody used in immunoprecipitation. **D,** Hippocampal levels of IGF-I after 2 hours of enriched housing in mice (n= 19-20). **E,** Hippocampal levels of pTyrIGF-I receptor after environmental enrichment. Four representative animals for each group are shown. Levels of pTyr IGF-I receptor were normalized with total IGF-I receptor. Densitometric analysis of normalized western blots is shown (n= 10; Student´s t-test, **p<0.001). **F,** Infusion of the IGF-I receptor antagonist PPP in the somatosensory cortex during unilateral tactile stimulation of the whiskers reduced neuronal activation in contralateral cortex. Upper: peristimulus time histograms of a representative S1 cortical neuron to whisker deflection (20 ms duration) in

control (left) and after 15 min of PPP (right). Lower: mean tactile responses to whisker deflections in S1 cortical neurons. PPP (solid bars), but not the vehicle (empty bars), reduced tactile responses (n= 19; **p=0.004).

Figure 2: Neuronal activation triggers entrance of circulating IGF-I. **A,** Panels **a&b**: digoxigenin immunostaining in somatosensory cortex of whisker-stimulated rats receiving an intracarotid injection of digoxigenin-IGF-I prior to stimulation (**a**); not stimulated rats (**b**). Note the presence of immunostaining in the stimulated side of the cortex. Dashed area indicates somatosensory cortex. No staining is observed in non-stimulated animals. Panel **c**: magnification of the square area in **a** (stimulated side)**.** Neuronal-like profiles and vessels appear stained. M1, primary motor cortex, S1BF, primary sensory cortex barrel field area. Panel **d**: digoxigenin-immunostaining in rat primary sensitive cortex in the area corresponding to hind limbs (S1HL) after sciatic nerve stimulation. Panel **e**: immunostaining with anti-digoxigenin shows a Dig-IGF-I accumulating neuron in the vicinity of an stained vessel in the somatosensory cortex after sciatic nerve stimulation. Panel **f**: magnification of the same cortical area in a different animal after sciatic nerve stimulation. Dig-immunopositive neuron-like cells and vessels are seen. Representative animals are shown. **B,** After whisker stimulation, double immunocytochemistry with anti-digoxigenin and cell-specific markers denoted co-staining of Dig-IGF-I in endothelial cells (tomato lectin^{+}), astrocytes (GFAP^{+}) and neurons ($\beta_3$tubulin^{+}) in the stimulated side. A small vessel in barrel cortex is shown. Astrocytes surrounding a large vessel are shown. **C;** Panels **a&b**: digoxigenin immunostaining in the dorsal thalamus of non-stimulated (**a**) and stimulated (**b**) rats. Panels **c&d**: magnification of the square areas in **a&b**. Note the increased number of stained neuron-like cells in the stimulated side. VPM, ventral postero-

medial thalamus, VPL, ventral postero-lateral thalamus, RET, reticular nucleus of the thalamus. **D,** Stimulated brain areas along the whisker-barrrel cortex pathway accumulate Dig-IGF-I. Neuronal activation determined by c-fos staining (green) showed overlapping of Dig-IGF-I staining (red) with active regions within this sensory pathway. Relay areas such as the sensitive nucleus of the trigeminal nerve, the lateral thalamus or the primary somatosensoty cortex are shown.

Figure 3: Systemically injected Dig-IGF-I localizes in barrel cortex endothelial cells and neurons of vibrissae-stimulated rats. **A,** Electron microscopy photomicrograph of a brain endothelial cell showing immunogold staining against digoxigenin in cytoplasm, mitochondria, and chromatin. Arrowhead: stained mitochondria in an adjacent cell. **B,** Immunogold staining in the cell nucleus, mitochondria and cytoplasm of a neuron. Inset: two labelled mitochondria are shown. M: mitochondria; L: Lumen; BL: Basal lamina. Scale bar A-B: 1 µm, b: 500 nm.

Figure 4: Activity-dependent entrance of circulating IGF-I into the brain. **A,** Time course changes in CBF in barrel cortex during whisker stimulation. Data are averaged at 5 min intervals and represented as relative changes versus pre-stimulation values (-10 ~ 0 min). * $p<0.05$ vs. Sham; # $p<0.05$ vs. 5Hz. **B**, hIGF-I in insterstitial fluid collected by microdyalisis from the somatosensory cortex was detectable only in whisker-stimulated animals. Experimental schedule employed in these experiments is shown in the upper panel. Infusion of TTX to inhibit neuronal activity in the somatosensory cortex of vibrissae-stimulated animals abrogated the increase in hIGF-I levels. Infusion of L-NAME to inhibit vasodilation also blocked the stimulus-elicited increase in hIGF-I. Infusion of an MMP9

inhibitor also resulted in inhibition of the uptake of serum IGF-I. A two-way ANOVA revealed a significant interaction ($F(8,26)=3.300$, $p<0.01$) and a significant effect of time ($F(2, 26)=11.80$, $p<0.001$). A post-hoc Tukey's showed a significant difference between baseline and stimulation only in the stimulated group ($p<0.01$). The stimulated group was also significantly different from sham-stimulated (#$p<0.05$ by Student´s t-test). ○ Sham (n=6); ■ stimulated (n=8); ▲stimulated+TTX (n=5); ▼stimulated+L-NAME (n=6); ◊ stimulated+MMP9 inhibitor (n=6).

Figure 5: Mechanisms involved in transcytosis of IGF-I across the blood-brain barrier (BBB). **A,** Upper blot: Neurons (Neuro), brain endothelial cells (Endo), and astrocytes (Astro) accumulate bhIGF-I in vitro. Lower blots: after eliminating membrane bound bhIGF-I with acid wash prior to cell lysis, uptake of bhIGF-I by the 3 types of cells was still observed. Endothelial cells appear to take up more IGF-I than either neurons or astrocytes, as seen after normalization with βactin. Synthetic bhIGF-I was loaded in the right lane. Micrographs: double immunostaining with anti-bhIGF-I and GFAP (astrocytes), $\beta_3$tubulin (neurons) and tomato lectin (endothelium) showed intracellular IGF-I staining in the 3 types of cells. **B,** In a double-chamber well, endothelial/astrocyte co-cultures in the upper chamber transport intact bhIGF-I to the lower chamber where neurons internalize it as evidenced by the presence of bhIGF-I in neuronal extracts. Scheme of experimental arrangement is shown. **C,** In the presence of active matrix metalloprotease 9 (MMP9a) but not inactive (MMP9i), significantly more bhIGF-I was endocytosed by endothelial cells. IGFBP-3 inhibited this effect. A similar effect was produced by PSA. **$p<0.01$ and ***$p<0.001$ vs control; n=5. **D,** IGFBP-3 is produced by endothelial cell cultures. IGFBP-3 and normal rat serum (NRS, that contains IGFBP-3) were run in parallel as controls. **E,**

Human endothelioma cells transfected with a dominant negative IGF-I receptor (DN-IGF-IR) endocytosed less bhIGF-I than mock-transfected cells. Representative blot of two experiments done in duplicate is shown. Quantitation histograms of internalized bhIGF-I shown in the right. Western blots of cell lysates for bIGF-I and IGF-IR/βactin were run separately in different membranes (**p<0.01; n=4). **F,** IGFBP-3 is cleaved by active (MMPa), but not inactive MMP9 (MMP9i). Western blot of IGFBP-3 after treatment with MMP9 or the vehicle. Intact recombinant IGFBP-3 was run in the right lane.

Figure 6: MMP9 is involved in passage of serum IGF-I across brain endothelium. **A,** Passage of bhIGF-I through astrocytes/brain endothelial cells co-cultures in double-chamber wells is modulated by IGFBP-3 and MMP9 in an opposite fashion. bhIGF-I and IGFBP-3 were placed in the "blood" side (upper chamber) whereas MMP9 was placed in the "brain" side (lower chamber). (n= 4; *p<0.05 and **p<0.01 vs lower chamber in controls). **B,** Transcytosis of bhIGF-I was stimulated by glutamate (100 µM), an effect inhibited with an MMP9 inhibitor (10 µM). (n= 7; **p<0.01). **C,** MMP9 is present in endothelial cells (upper zymography and blot) and is stimulated by glutamate in endothelial-astrocyte co-cultures (lower zymography)**.** Representative experiments are shown (n=2-3). Glut: glutamate, MMPa: active synthetic MMP9 was run as a control. **D,** Active MMP9 is increased in the stimulated somatosensory cortex. Western blot of MMP9 in stimulated (stim) and unstimulated (unstim) cortex of the same animal . Recombinant MMP9 was run in parallel.

Figure 7: Mediators involved in neuro-vascular coupling modulate passage of blood-borne IGF-I across brain endothelium. **A,** Diffusible mediators released by astrocytes during

neuro-vascular coupling stimulated endocytosis of bhIGF-I by brain endothelial cells. Prostaglandin E_2 (PGE_2), epoxyeicosatrienoic acid (EET), and ATP, but not NO (stimulated with SNAP), enhanced IGF-I internalization. Combined addition of the 3 compounds elicited a similar increase (n=6-10). **B,** Infusion of PGE_2 into the cerebral cortex (-0.5 mm from bregma, 1 mm depth) of rats previously receiving an intra-carotid injection of Dig-IGF-I results in robust digoxigenin staining in the infused side 30 min later. Note that both the contralateral, vehicle-infused side and the brain surface of the injected side showed low immunoreactivity attributable to local disruption of the BBB. Three consecutive 50 μm brain sections are shown. **C,** Enhanced internalization of bhIGF-I by PGE_2, EET, and ATP is inhibited by the MMP9 inhibitor. Note that the drug alone decreases bhIGF-I internalization to the same extent, indicating that endogenous MMP9 is required to internalize IGF-I (n= at least 3 experiments), ***$p<0.001$, **$p<0.01$, and *$p<0.05$ vs control.

Figure 8: The IGF-I receptor interacts with LRP-1 in brain endothelial cells. **A,** LRP-1 co-immunoprecipitates with IGFBP-3. Standard IGFBP-3 is shown in the right lane. **B,** Co-immunoprecipitation of LRP1 and IGF-I receptors in brain endothelial cells. An LRP1 band was detected only in anti-IGF-I receptor (IGF-IR) immunoprecipitates (IP). Sup: supernatants. **C,** IGF-I receptors (IGF-IR) in brain endothelial cells co-immunoprecipitated with an HA-tagged mini-LRP1. Both supernatants (Sup) and immunoprecipitated pellets (IP) were assayed in an IGF-IR western blot. Controls included non-transfected cells and anti-IGF-IR immunoprecipitated fractions. **D,** Transfection of brain endothelial cells with mini-LRP1 enhanced endocytosis of bhIGF-I (**$p<0.01$, n= 4). **E,F,** Transfection of the human endothelioma HCMEC-D3 with an LRP1 siRNA resulted in marked inhibition of

bhIGF-I internalization**.** Control cultures were transfected with a scramble shRNA sequence. E: Western blots of cell lysates for bIGF-I and LRP1/βactin were run separately in different membranes. Two experiments (in duplicate) were loaded/gel. F: Quantitation histograms (*$p<0.05$; n=4). **G,** Proposed mechanisms involved in serum IGF-I uptake by active brain regions. Increased neuronal activaty results in increased blood flow through neuro-vascular coupling. The resulting local vasodilation increases the amount of circulating IGF-I at the stimulated area. Neuronal activity also stimulates MMP9 activity that releases IGF-I from IGFBP3 allowing its internalization through the BBB in an LRP1-dependent process. Increased IGF-I input in stimulated areas stimulates neuronal activity Through this step-wise pathway serum IGF-I could modulate neuronal activity.

Acknowledgements We are thankful to I. Alvarez, M. Garcia, M. Oliva and L Guinea for technical support and L. Genis and A. Trueba for help with the cell cultures. This work was funded by Spanish Ministry of Science (SAF2007-60051), by CIBERNED and by a joint Japan-Spain collaborative program (JSPS-CSIC-2006JP0010).

Experimental procedures

Stimulation protocols. Different types of brain stimulation protocols were used. In a first type rats were anesthetized with urethane (1.1 g/kg i.p.) and the anesthesia maintained with intermittent injections (approximately 0.1 g/kg/h). The trachea was cannulated and ventilated with ambient air. Body temperature (37ºC), respiration rate (20 cycles/min) and end-tidal CO2 percentage were monitored and controlled. One carotid artery was cannulated with PE-50 polyethylene tubing for hIGF-I injection (10 ug/100 grs). Electrical stimulation of the inferior cerebellar peduncle was carried out with twisted teflon coated wires inserted in the following coordinates: AP: -11 mm; L: 3 mm; DV: 5 mm from the surface. Stimulus was a 0.1 ms square pulse (50-100 μA) at 5 Hz frequency. Stimulus evoked potentials were recorded in the ipsilateral cerebellum in several animals to confirm the stimulation. In a second type of protocol the rat whisker pad was stimulated with two subcutaneous electrodes (0.3 mm diameter, stainless steel) located at the dorso-anterior and caudo-posterior edges of the whisker pad. Stimulus was a 1ms square pulse applied at twice the intensity necessary to elicit visible movement of the whiskers (50-100 μA). Such intensity did not induce movement in the whiskers of the contralateral pad. In some experiments, stimulus evoked potentials were recorded in barrel cortex at the following coordinates: AP: -3 mm from bregma; L: 5 mm from midline; DV: 1 mm from the brain surface. In a third type of protocol the whiskers were stimulated by an electronically gated, short-lasting air jet (1Kg/ cm2, 20 ms of duration) which could be directed to an individual whisker. The control tactile stimulation consisted in pulses lasting 20 ms and delivered at 0.5 Hz. In an additional protocol animals were anesthesized with urethane (1.6 gr/kg) and their sciatic nerve stimulated by exposing the popliteum fosae and delivering pulses of 100

μs and 0.5 Hz with a square pulse generator (Grass S88). Stimulation intensity was adjusted to twice the amount needed to elicit muscle contractions (10-50 μA). For sham stimulation, electrodes were placed without delivering any current.

Behavioral stimulation was produced by placing during 2 hours adult male mice in an enriched housing consisting of a large arena containing different toys, plastic tunnels, exercise wheels and 10 animals. Non-stimulated animals remained in their standard laboratory cages.

Brain microdialysis. Rats were anesthetized with sodium pentobarbital (50 mg/kg, ip) and fixed to a stereotaxic frame. A guide cannula for microdialysis was placed onto the intact duramater above the barrel cortex (coordinates: AP -1.8 mm, L 5.5 mm) contralateral to the stimulated whisker pad, and fixed to the skull. After surgery, the rats were housed individually and allowed to recover for at least two days. Approximately 24h before the experiment, a needle was inserted through the guide cannula to punch the duramater, then a microdialysis probe (Eicom, Japan; cutoff of 1,000 kDa; membrane length 2.0 mm; outer diameter 0.6 mm) was inserted into the barrel cortex. The probe was infused with artificial cerebrospinal fluid (aCSF, Harvard Apparatus, USA) in a push-pull manner with a micro-pump at 2.5 μl/min. After a 60 min stabilization period, dialysates were collected at 60 min intervals for baseline, stimulation, and post-stimulation period (each sample containing 150 ul dialysate). Five minutes before starting whisker pad stimulation at 2 Hz, hIGF-I (50 μg/100μl saline) was injected into the carotid artery. The following drugs were used: tetradotoxin (TTX, a sodium channel blocker, Tocris, 2 μM), the NO synthase inhibitor, L-NAME (Tocris, 200 μM) and a MMP-9 inhibitor (Calbiochem, 10 μM). Drugs were administered from 60 min before the baseline sampling, and continued throughout the

experiment (see FigS3C for an schematic of this protocol). At the end of the experiment, the brain was removed and fixed with 4% paraformaldehyde, and cannula placement confirmed by histology. The dialysates were stored at -80°C until IGF-I content was measured. As circulating hIGF-I could non-specifically enter into the brain through disruption of the blood-brain barrier with the microdyalisis probe we checked BBB integrity by injecting Evans blue. We observed very limited disruption in the brain surface while the area surrounding the tip of the probe remained intact (not shown).

Cell cultures and in vitro assays. Endothelial cell cultures were performed as described (Perriere et al., 2007). Briefly, brains were dissected free of meninges on ice and phosphate buffer saline (NaCl, 137mM; KCl, 2.7mM; Na_2HPO_4, 1.5mM), and minced. Brain fragments were homogenized and digested for 1.5h at 37ºC in collagenase/dispase (270U collagenase/ml, 0.1% dispase) and DNAse (10U/ml) in DMEM. Cells were centrifuged and the pellet resuspended in 20% fetal bovine serum /DMEM (1000g, 15 min) and incubated in the collagenase/dispase mixture for 1h at 37ºC. The capillary fragments were retained on a 10 μm nylon filter, and endothelial cells removed from the filter with endothelial cell basal medium supplemented with 20% fetal bovine serum and antibiotics (penicillin, 100 U/ml, streptomycin, 100 μg/ml). Cells were seeded in plates coated with collagen type IV (5 μg/cm3). Puromycin (3μg/ml) was added for 3 days and replaced by fibroblast growth factor (2 ng/ml) and hydrocortisone (500 ng/ml). Astrocyte and neuronal cultures were performed as described (Fernandez et al., 2007). Astrocytes were grown in DMEM + 10% serum. Co-culture of endothelial cells and astrocytes was performed as described elsewhere (Perriere et al., 2007). Three weeks after seeding, astrocytes were trypsinized at 37ºC, 5 min and seeded (5x104 cells) on collagen VI/fibronectin (0.1 mg/ml and 0.05 mg/ml,

respectively)- coated Transwell polyester inserts in DMEM +10% serum. One day after seeding, wells were washed and endothelial cells plated on top of the astrocyte layer. Endothelial cells were obtained by trypsinizing endothelial cultures four days after initial seeding. Under these culture conditions formation of a sealed monolayer mimicking brain barrier properties was confirmed by measuring electrical resistance: >100 Ω/cm^2, and retention of fluorescent dextran in the upper chamber. Human endothelioma HCMEC-D3 cells were cultured in DMEM-F12 + 10% FCS.

Transcytosis assays were performed one week later using biotinylated IGF-I (0.2 μg/ml) to distinguish it from endogenously produced IGF-I. bhIGF-I was added to double chamber cultures for 1-5 hours before collecting the medium. Internalization assays in cell monolayers were performed adding bhIGF-I (0.2 μg/ml) to the respective cultures for 30 min and washing 3 times with PBS before collection of the cells. To rule out unspecific binding of bhIGF-I to cell membranes, cells were exposed to 40 ng/ml of bhIGF-I for 30 min followed by two washes with 0.1 M PBS pH 6.0 and incubation in EDTA-lysis buffer + protease inhibitors /4ºC for 5 min. Analysis of bhIGF-I content in cells (internalization assays) and culture medium (transcytosis assays) was performed by western blot using horseradise peroxidase-coupled streptavydin. Transfection of cells with siRNA against LRP1, scramble siRNA (Sigma), mini-LRP1, or dominant negative IGF-I receptor was carried out with Fugene 6 (Roche). Cells were used 48-72 h after transfection. In experiments with inhibitory drugs or IGFBP3, cells were incubated with the different compounds 20-60 min prior to the respective experiment. Inhibitory drugs used to assess their effects on glutamate-induced IGF-I transfer were added 45 min ahead of glutamate. Activation of MMPs was carried out by incubating at a ratio of 1:10 APMA 10nM (in NaOH 0.1M) with the corresponding MMP for 1 hour/37ºC before adding them to the cells.

Statistics. A two-way ANOVA was used for overall comparisons and one-way ANOVA for intra-group comparisons. Post-hoc tests used included Tukey and Student´s t-test. Statistics (microdialysis experiments).

Please see supplemental information for the following experimental procedures: animals and materials, in vivo procedures, cerebral blood-flow measurements, in vivo recordings, immunoassays, gel zymography, pre-embedding immunogold labeling and EM, and quantitative PCR,

Table 1. Changes in arterial blood parameters and body temperature at pre- and post stimulations.

	Pre		Post		
	Mean	**SE**	**Mean**	**SE**	
Control					
pH	7.43	0.01	7.43	0.01	n.s.
PCO2 (mmHg)	36.0	1.4	38.2	0.6	n.s.
PO2 (mmHg)	96.2	2.3	94.6	2.8	n.s.
Mean Arterial Pressure (mmHg)	98.5	3.8	100.1	4.4	n.s.
Heart Rate (bpm)	371	6.1	375	6.5	n.s.
Body Temperature (°C)	37.6	0.2	37.7	0.1	n.s.
2Hz					
pH	7.44	0.00	7.43	0.01	n.s.
PCO2 (mmHg)	36.3	2.5	38.0	2.4	n.s.
PO2 (mmHg)	89.9	1.7	89.7	5.2	n.s.
Mean Arterial Pressure (mmHg)	93.2	5.9	98.5	3.0	n.s.
Heart Rate (bpm)	349	5.2	358	6.1	n.s.
Body Temperature (°C)	37.7	0.3	37.5	0.2	n.s.
5Hz					
pH	7.44	0.01	7.42	0.01	n.s.
PCO_2 (mmHg)	38.3	1.0	38.1	0.9	n.s.
PO_2 (mmHg)	89.7	3.2	90.2	2.2	n.s.
Mean Arterial Pressure (mmHg)	90.4	4.1	91.4	4.8	n.s.
Heart Rate (bpm)	382	18.8	391	13.2	n.s.
Body Temperature (°C)	37.7	0.2	37.4	0.1	n.s.

n = 4-5. n.s., non significant (paired t-test).

Table 2. Glutamate-dependent pathways involved in transcytosis of IGF-I across endothelial-astrocyte co-cultures in double-chamber configuration.

Treatment	**IGF-I transcytosis**[a] (% glutamate)	**Statistical significance**[b]
Glutamate (n=5)	100 ± 26	-[c]
Glutamate + AP5 (n=5)	73 ± 31	0.24
Glutamate + CNQX (n=5)	55 ± 11	0.001
Glutamate + Lyly (n=5)	184 ± 120	0.33
Glutamate + MPEP (n=3)	0.3 ± 0.19	0.0004
Glutamate + Thapsigargin (n=3)	0.2 ± 0.5	0.0003
Glutamate + EGTA (n=3)	5.1 ± 0.4	0.0006
Glutamate + Ibuprofen (n=3)	53 ± 21	0.002
Glutamate + Suramin (n=3)	113 ± 18	0.13

[a] Mean ± SEM

[b] As compared to glutamate (Student´s t-test)

[c] Glutamate induced a 217 ± 58% increase in IGF-I transcytosis over controls (p=0.02).

Reference List

Abbott,N.J., Patabendige,A.A.K., Dolman,D.E.M., Yusof,S.R., and Begley,D.J. (2010). Structure and function of the blood-brain barrier. Neurobiology of Disease *37*, 13-25.

Aberg,M.A., Aberg,N.D., Hedbacker,H., Oscarsson,J., and Eriksson,P.S. (2000). Peripheral infusion of IGF-I selectively induces neurogenesis in the adult rat hippocampus. J. Neurosci. *20*, 2896-2903.

Arwert,L.I., Veltman,D.J., Deijen,J.B., Lammertsma,A.A., Jonker,C., and Drent,M.L. (2005). Memory performance and the growth hormone/insulin-like growth factor axis in elderly: a positron emission tomography study. Neuroendocrinology *81*, 31-40.

Auletta,M., Nielsen,F.C., and Gammeltoft,S. (1992). Receptor-mediated endocytosis and degradation of insulin-like growth factor I and II in neonatal rat astrocytes. J. Neurosci. Res. *31*, 14-20.

Banks,W.A. Mouse models of neurological disorders: A view from the blood-brain barrier. Biochimica et Biophysica Acta (BBA) - Molecular Basis of Disease *In Press, Corrected Proof*.

Banks,W.A. (2006). Denial Versus Dualism: The Blood-Brain Barrier as an Interface of the Gut-Brain Axis. Endocrinology *147*, 2609-2610.

Bilodeau,N., Fiset,A., Boulanger,M.C., Bhardwaj,S., Winstall,E., Lavoie,J.N., and Faure,R.L. (2009). Proteomic Analysis of Src Family Kinases Signaling Complexes in Golgi/Endosomal Fractions Using a Site-Selective Anti-Phosphotyrosine Antibody: Identification of LRP1-Insulin Receptor Complexes. J Proteome. Res.

Carro,E., Nunez,A., Busiguina,S., and Torres-Aleman,I. (2000). Circulating insulin-like growth factor I mediates effects of exercise on the brain. J. Neurosci. *20*, 2926-2933.

Carro,E., Trejo,J.L., Nunez,A., and Torres-Aleman,I. (2003). Brain repair and neuroprotection by serum insulin-like growth factor I. Mol. Neurobiol. *27*, 153-162.

Carro,E., Spuch,C., Trejo,J.L., Antequera,D., and Torres-Aleman,I. (2005). Choroid Plexus Megalin Is Involved in Neuroprotection by Serum Insulin-Like Growth Factor I. J. Neurosci. *25*, 10884-10893.

Chung,S., Li,X., and Nelson,S.B. (2002). Short-term depression at thalamocortical synapses contributes to rapid adaptation of cortical sensory responses in vivo. Neuron *34*, 437-446.

Ciucci,F., Putignano,E., Baroncelli,L., Landi,S., Berardi,N., and Maffei,L. (2007). Insulin-Like Growth Factor 1 (IGF-1) Mediates the Effects of Enriched Environment (EE) on Visual Cortical Development. PLoS. ONE. *2*, e475.

Dietrich,M.O., Spuch,C., Antequera,D., Rodal,I., de Yebenes,J.G., Molina,J.A., Bermejo,F., and Carro,E. (2007). Megalin mediates the transport of leptin across the blood-CSF barrier. Neurobiol. Aging.

Fernandez,A.M., Fernandez,S., Carrero,P., Garcia-Garcia,M., and Torres-Aleman,I. (2007). Calcineurin in reactive astrocytes plays a key role in the interplay between proinflammatory and anti-inflammatory signals. J Neurosci *27*, 8745-8756.

Fratiglioni,L., Paillard-Borg,S., and Winblad,B. (2004). An active and socially integrated lifestyle in late life might protect against dementia. Lancet Neurol. *3*, 343-353.

Garcia-Segura,L.M., Perez,J., Pons,S., Rejas,M.T., and Torres-Aleman,I. (1991). Localization of insulin-like growth factor I (IGF-I)-like immunoreactivity in the developing and adult rat brain. Brain Res. *560*, 167-174.

Geary,E.S., Rosenfeld,R.G., and Hoffman,A.R. (1989). Insulin-like growth factor-I is internalized after binding to the type I insulin-like growth factor receptor. Horm. Metab Res. *21*, 1-3.

Guzzetta,A., Baldini,S., Bancale,A., Baroncelli,L., Ciucci,F., Ghirri,P., Putignano,E., Sale,A., Viegi,A., Berardi,N., Boldrini,A., Cioni,G., and Maffei,L. (2009). Massage accelerates brain development and the maturation of visual function. J Neurosci *29*, 6042-6051.

Harder,D.R., Alkayed,N.J., Lange,A.R., Gebremedhin,D., and Roman,R.J. (1998). Functional hyperemia in the brain: hypothesis for astrocyte-derived vasodilator metabolites. Stroke *29*, 229-234.

Haydon,P.G., and Carmignoto,G. (2006). Astrocyte control of synaptic transmission and neurovascular coupling. Physiol Rev *86*, 1009-1031.

Huang,S.S., Ling,T.Y., Tseng,W.F., Huang,Y.H., Tang,F.M., Leal,S.M., and Huang,J.S. (2003). Cellular growth inhibition by IGFBP-3 and TGF-beta1 requires LRP-1. FASEB J. *17*, 2068-2081.

Iadecola,C., and Nedergaard,M. (2007). Glial regulation of the cerebral microvasculature. Nat Neurosci *10*, 1369-1376.

Kaelin-Lang,A. (2008). Enhancing rehabilitation of motor deficits with peripheral nerve stimulation. NeuroRehabilitation. *23*, 89-93.

Kempermann,G. (2002). Regulation of adult hippocampal neurogenesis - implications for novel theories of major depression. Bipolar. Disord. *4*, 17-33.

Lee,W.H., Wang,G.M., Yang,X.L., Seaman,L.B., and Vannucci,S.I. (1999). Perinatal hypoxia-ischemia decreased neuronal but increased cerebral vascular endothelial IGFBP3 expression. Endocrine. *11*, 181-188.

Leveille,F., Papadia,S., Fricker,M., Bell,K.F.S., Soriano,F.X., Martel,M.A., Puddifoot,C., Habel,M., Wyllie,D.J., Ikonomidou,C., Tolkovsky,A.M., and Hardingham,G.E. (2010). Suppression of the Intrinsic Apoptosis Pathway by Synaptic Activity. J. Neurosci. *30*, 2623-2635.

Lopez-Lopez,C., LeRoith,D., and Torres-Aleman,I. (2004). Insulin-like growth factor I is required for vessel remodeling in the adult brain. Proc. Natl. Acad. Sci. U. S. A *101*, 9833-9838.

Manes,S., Llorente,M., Lacalle,R.A., Gomez-Mouton,C., Kremer,L., Mira,E., and Martinez,A. (1999). The matrix metalloproteinase-9 regulates the insulin-like growth factor-triggered autocrine response in DU-145 carcinoma cells. J. Biol. Chem. *274*, 6935-6945.

Marks,J.L., Porte,D., Jr., and Baskin,D.G. (1991). Localization of type I insulin-like growth factor receptor messenger RNA in the adult rat brain by in situ hybridization. Mol. Endocrinol. *5*, 1158-1168.

Michaluk,P., and Kaczmarek,L. (2007). Matrix metalloproteinase-9 in glutamate-dependent adult brain function and dysfunction. Cell Death. Differ. *14*, 1255-1258.

Moore,C.I., and Cao,R. (2007). The Hemo-Neural Hypothesis: On The Role of Blood Flow in Information Processing. J Neurophysiol 01366.

Nunez,A., Carro,E., and Torres-Aleman,I. (2003). Insulin-like growth factor I modifies electrophysiological properties of rat brain stem neurons. J. Neurophysiol. *89*, 3008-3017.

Papadia,S., Soriano,F.X., Leveille,F., Martel,M.A., Dakin,K.A., Hansen,H.H., Kaindl,A., Sifringer,M., Fowler,J., Stefovska,V., Mckenzie,G., Craigon,M., Corriveau,R., Ghazal,P., Horsburgh,K., Yankner,B.A., Wyllie,D.J.A., Ikonomidou,C., and Hardingham,G.E. (2008). Synaptic NMDA receptor activity boosts intrinsic antioxidant defenses. Nat Neurosci *11*, 476-487.

Pardridge,W.M. (1993). Transport of insulin-related peptides and glucose across the blood-brain barrier. Ann. N. Y. Acad. Sci. *692*, 126-137.

Perea,G., Navarrete,M., and Araque,A. (2009). Tripartite synapses: astrocytes process and control synaptic information. Trends Neurosci *32*, 421-431.

Perriere,N., Yousif,S., Cazaubon,S., Chaverot,N., Bourasset,F., Cisternino,S., Decleves,X., Hori,S., Terasaki,T., Deli,M., Scherrmann,J.M., Temsamani,J., Roux,F., and Couraud,P.O. (2007). A functional in vitro model of rat blood-brain barrier for molecular analysis of efflux transporters. Brain Res. *1150*, 1-13.

Pulford,B.E., and Ishii,D.N. (2001). Uptake of circulating insulin-like growth factors (IGFs) into cerebrospinal fluid appears to be independent of the IGF receptors as well as IGF-binding proteins. Endocrinology *142*, 213-220.

Reinhardt,R.R., and Bondy,C.A. (1994). Insulin-like growth factors cross the blood-brain barrier. Endocrinology *135*, 1753-1761.

Roy,C.S., and Sherrington,C.S. (1890). On the Regulation of the Blood-supply of the Brain. J Physiol *11*, 85-158.

Russo,V.C., Gluckman,P.D., Feldman,E.L., and Werther,G.A. (2005). The Insulin-Like Growth Factor System and Its Pleiotropic Functions in Brain. Endocr Rev *26*, 916-943.

Sehat,B., Tofigh,A., Lin,Y., Trocme,E., Liljedahl,U., Lagergren,J., and Larsson,O. (2010). SUMOylation Mediates the Nuclear Translocation and Signaling of the IGF-1 Receptor. Sci Signal. *3*, ra10.

Shi,Y., Liu,X., Gebremedhin,D., Falck,J.R., Harder,D.R., and Koehler,R.C. (2008). Interaction of mechanisms involving epoxyeicosatrienoic acids, adenosine receptors, and metabotropic glutamate receptors in neurovascular coupling in rat whisker barrel cortex. J Cereb Blood Flow Metab *28*, 111-125.

Trejo,J.L., Llorens-Martin,M.V., and Torres-Aleman,I. (2008). The effects of exercise on spatial learning and anxiety-like behavior are mediated by an IGF-I-dependent mechanism related to hippocampal neurogenesis. Mol Cell Neurosci *37*, 402-411.

Trejo,J., Piriz,J., Llorens-Martin,M.V., Fernandez,A.M., Bolos,M., LeRoith,D., Nunez,A., and Torres-Aleman,I. (2007). Central actions of liver-derived insulin-like growth factor I underlying its pro-cognitive effects. Mol Psychiatry *12*, 1118-1128.

Wang,L., Zhang,Z.G., Zhang,R.L., Gregg,S.R., Hozeska-Solgot,A., LeTourneau,Y., Wang,Y., and Chopp,M. (2006). Matrix metalloproteinase 2 (MMP2) and MMP9 secreted by erythropoietin-activated endothelial cells promote neural progenitor cell migration. J Neurosci *26*, 5996-6003.

Zapf,A., Hsu,D., and Olefsky,J.M. (1994). Comparison of the intracellular itineraries of insulin-like growth factor-I and insulin and their receptors in Rat-1 fibroblasts. Endocrinology *134*, 2445-2452.

Zonta,M., Angulo,M.C., Gobbo,S., Rosengarten,B., Hossmann,K.A., Pozzan,T., and Carmignoto,G. (2003). Neuron-to-astrocyte signaling is central to the dynamic control of brain microcirculation. Nat Neurosci *6*, 43-50.

Figure

Click here to download high resolution image

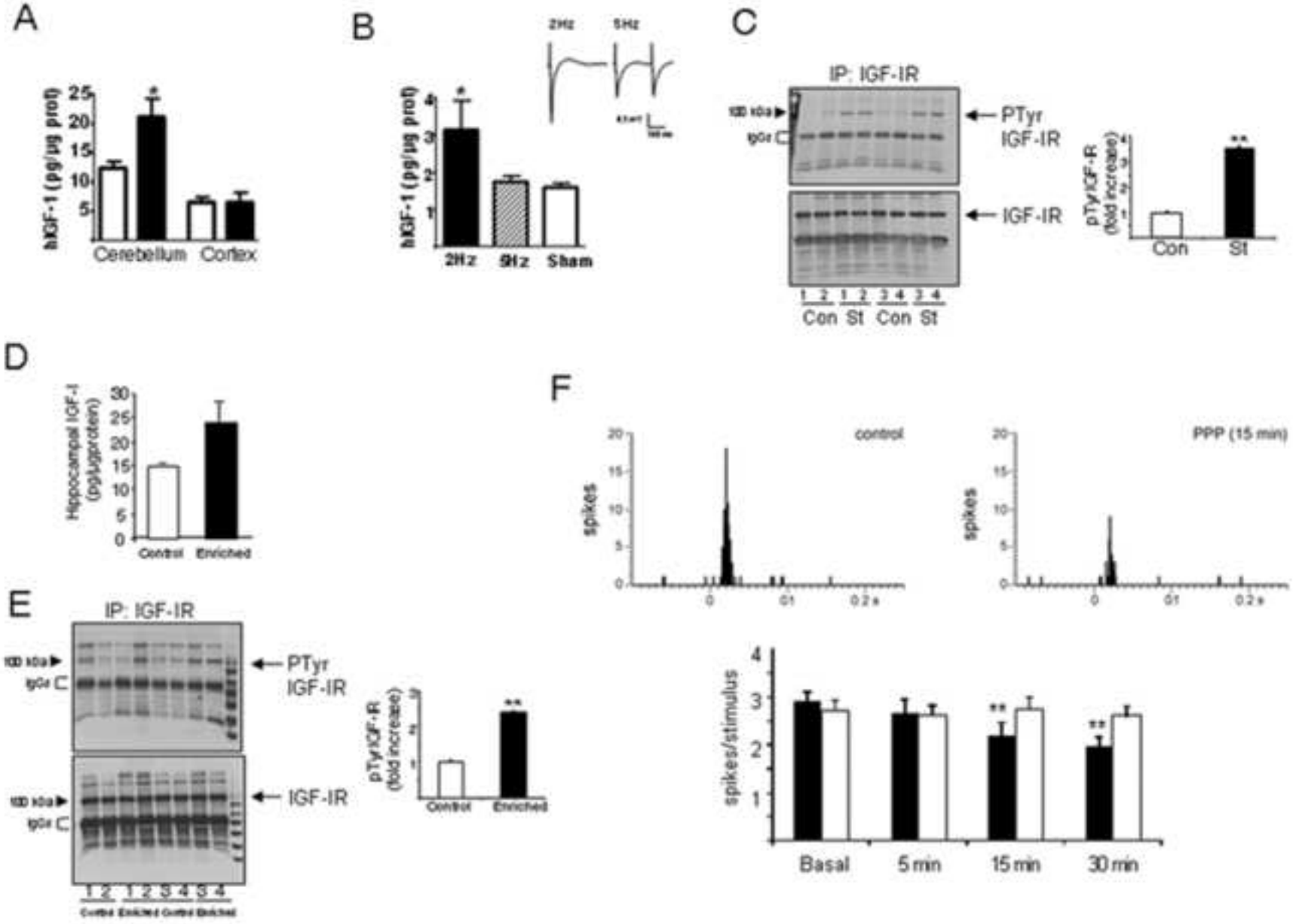

Figure 1

Figure 2

Click here to download high resolution image

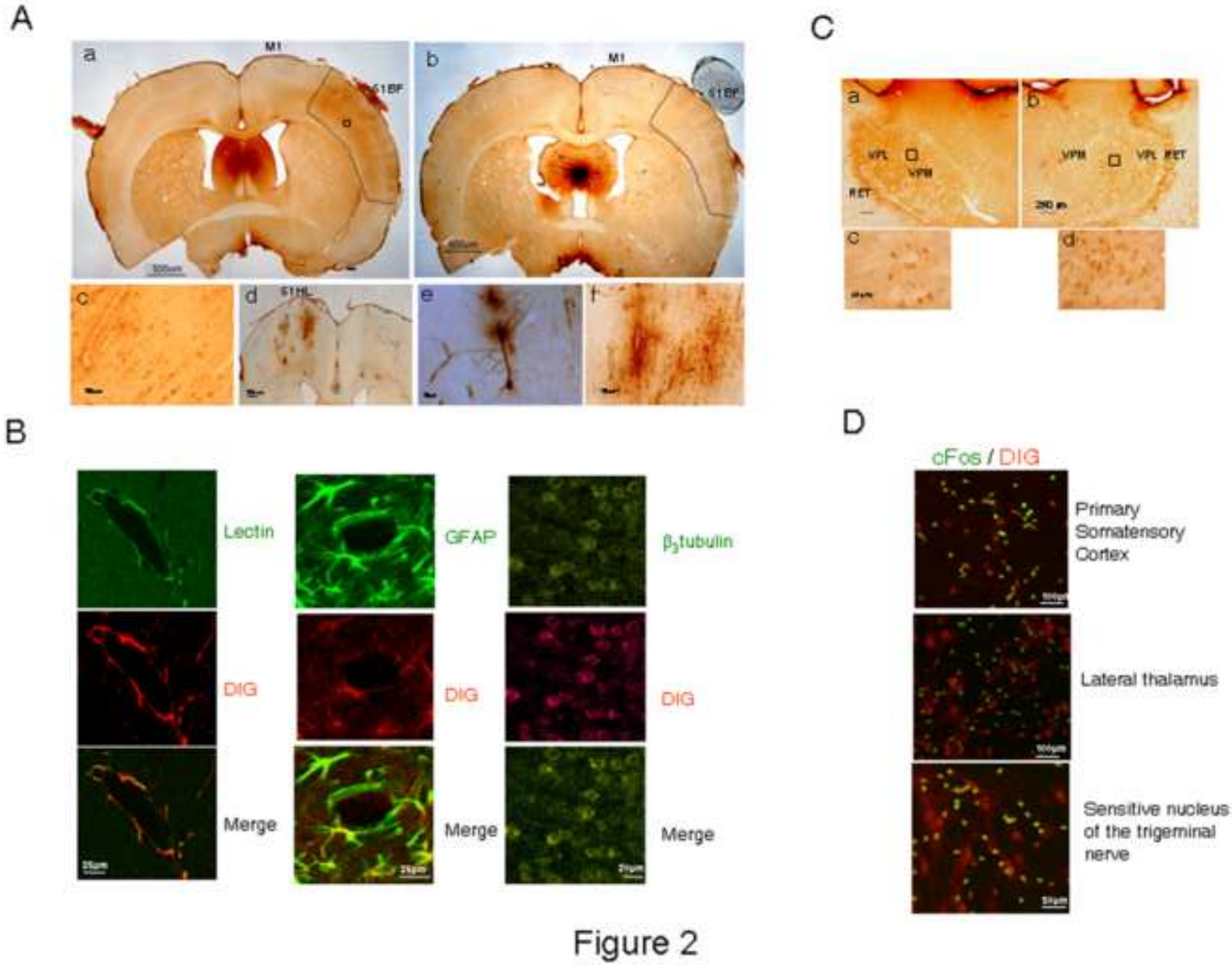

Figure 2

Figure 3

Click here to download high resolution image

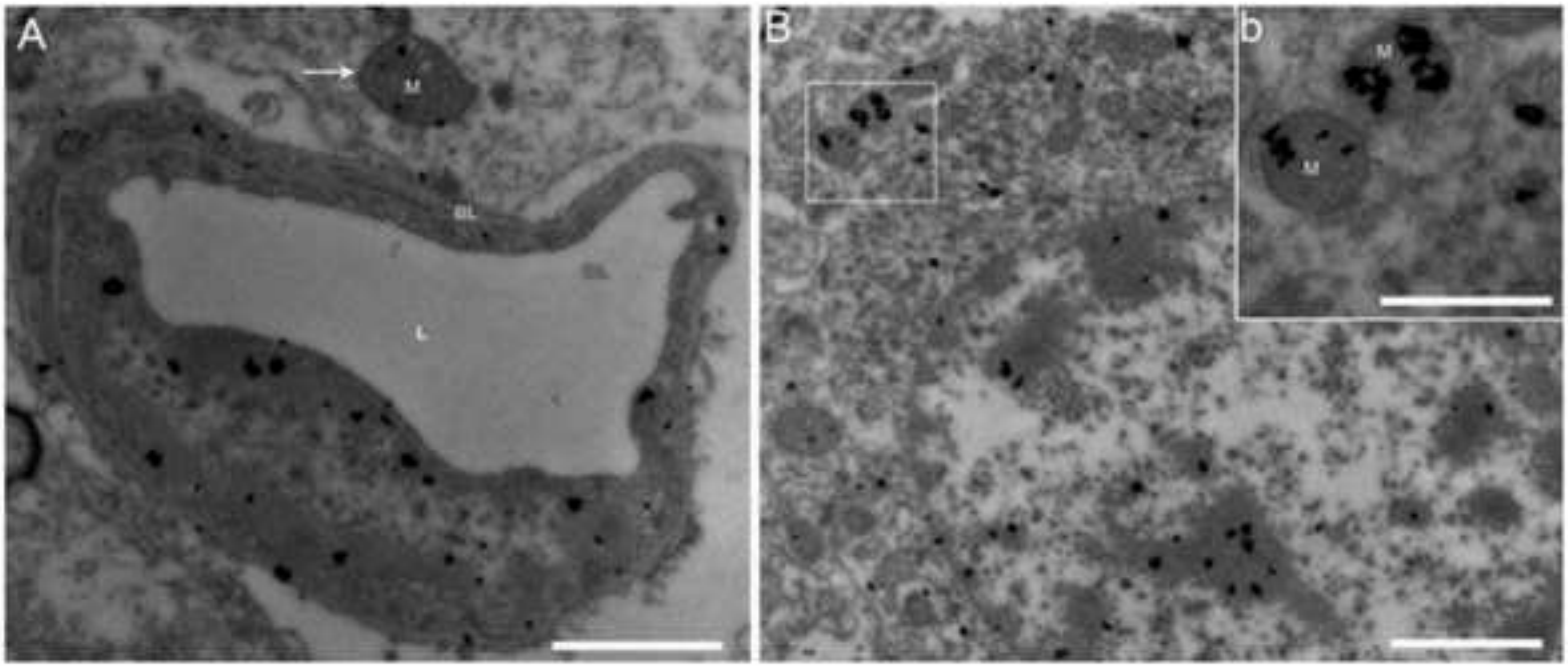

Figure 3

Figure 4

Click here to download high resolution image

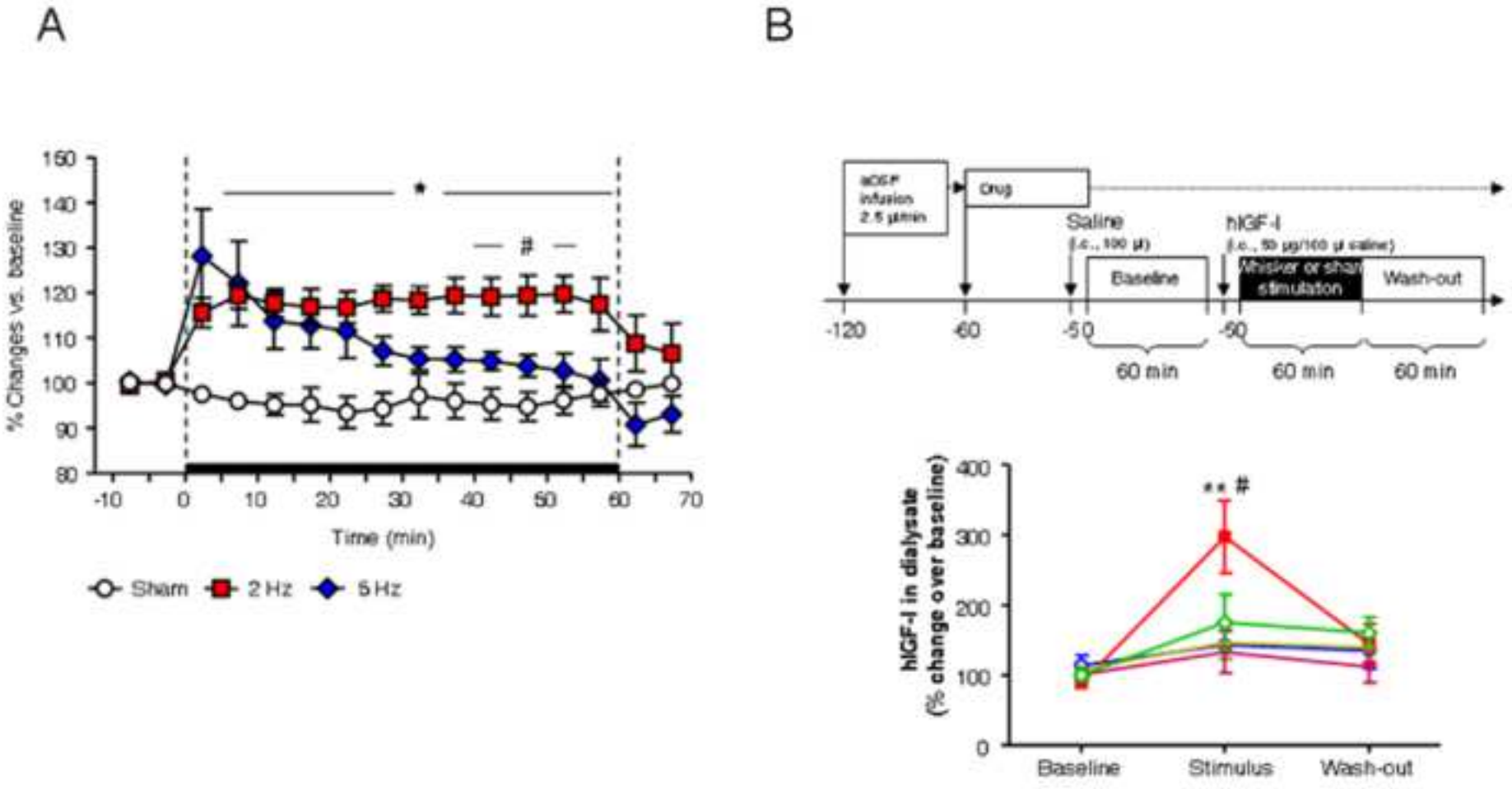

Figure 4

Figure 5

Click here to download high resolution image

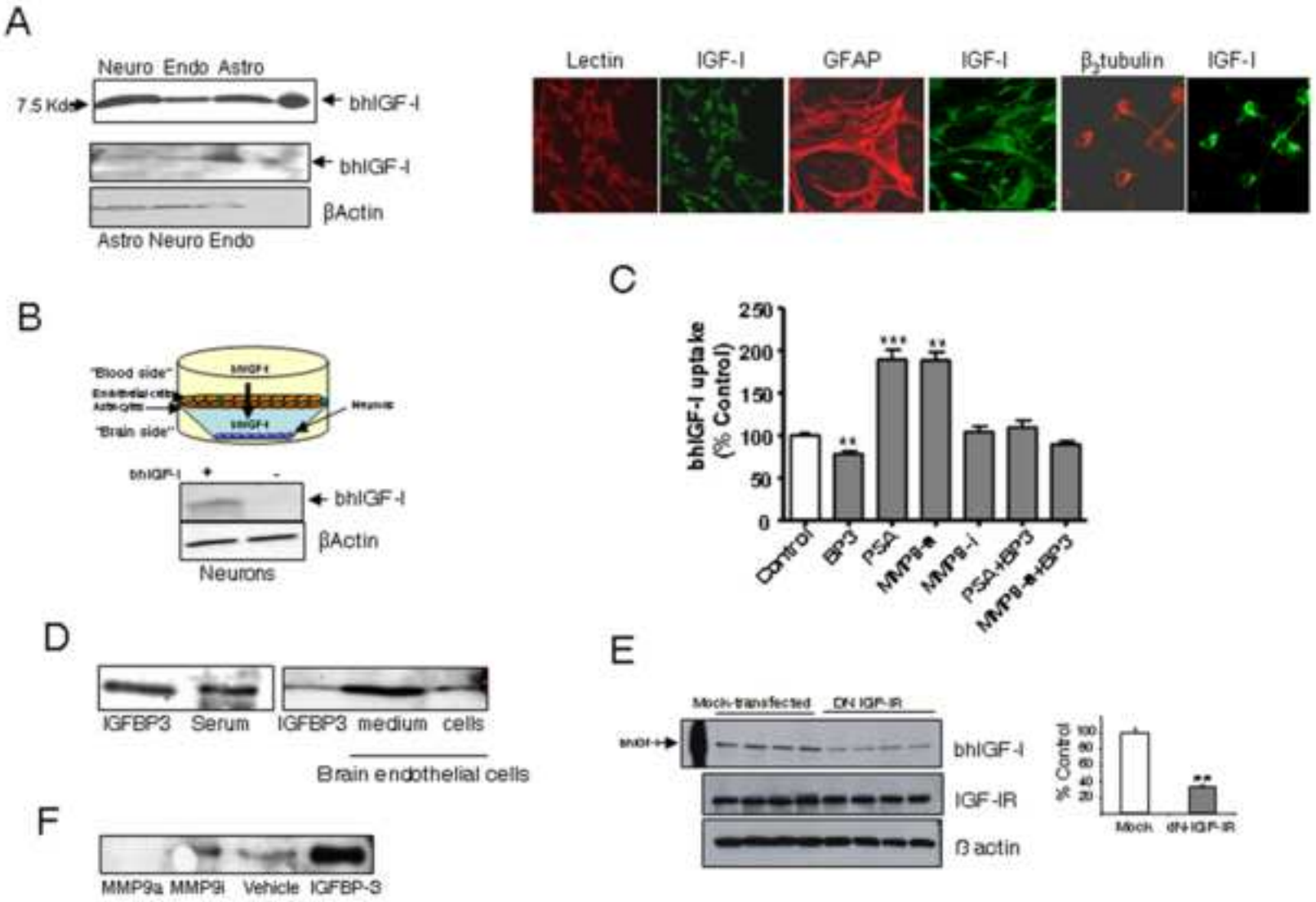

Figure 5

Figure 6

Click here to download high resolution image

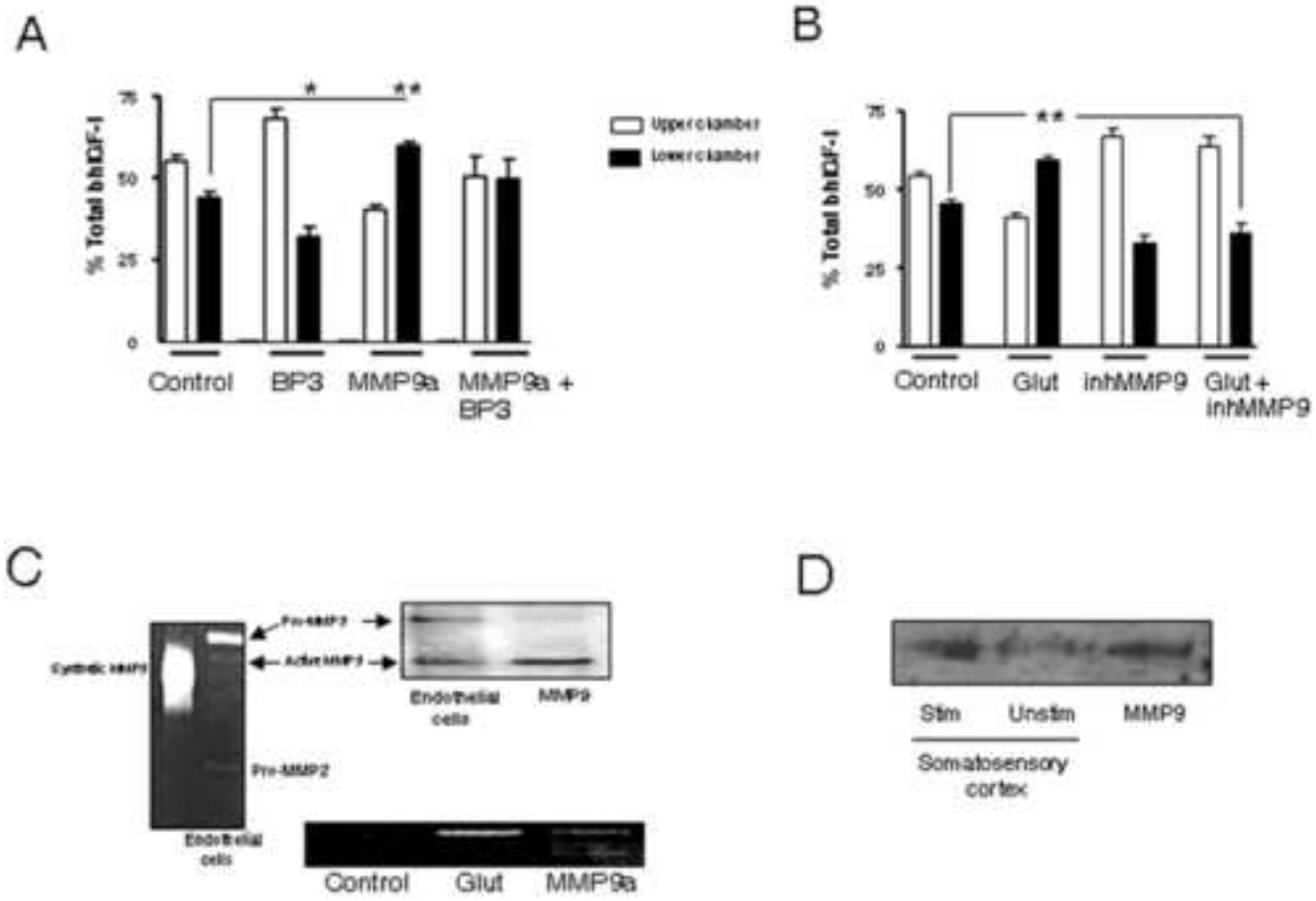

Figure 6

Figure 7

Click here to download high resolution image

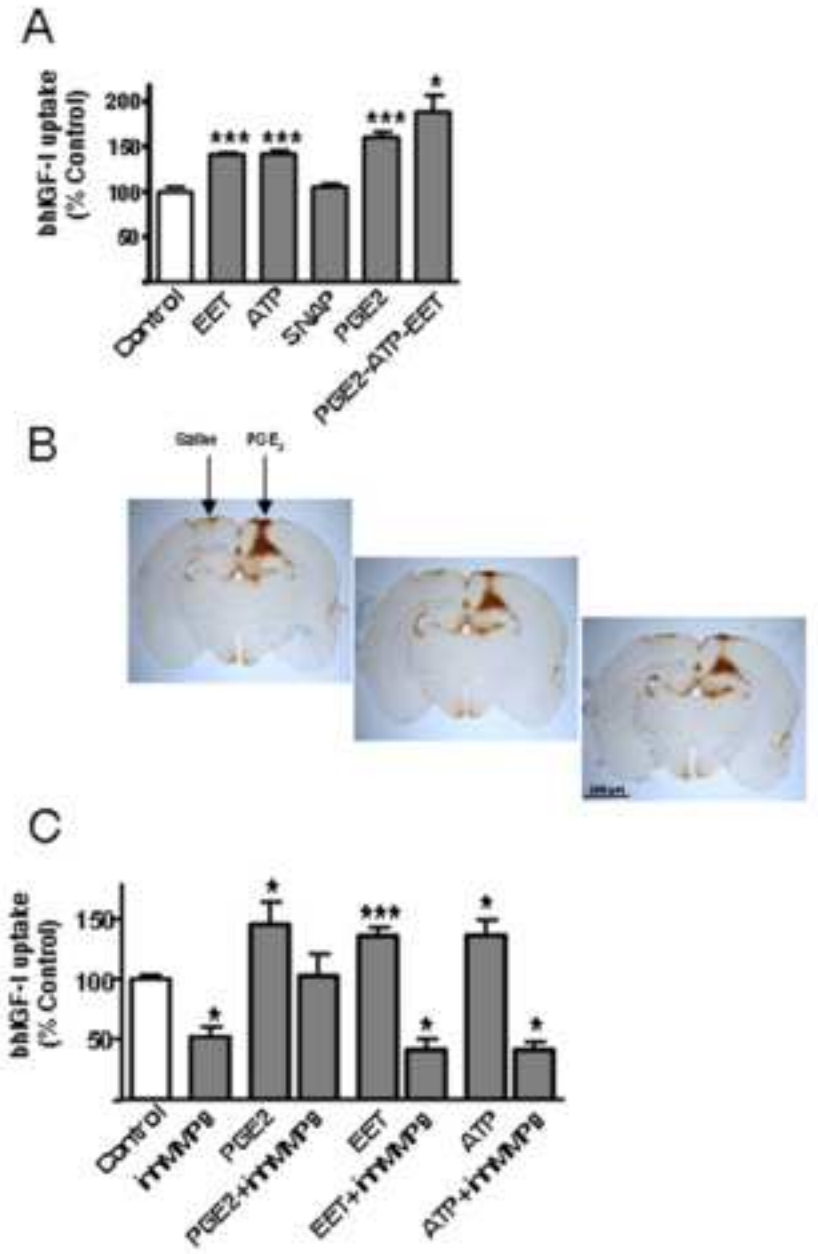

Figure 7

Figure 8

Click here to download high resolution image

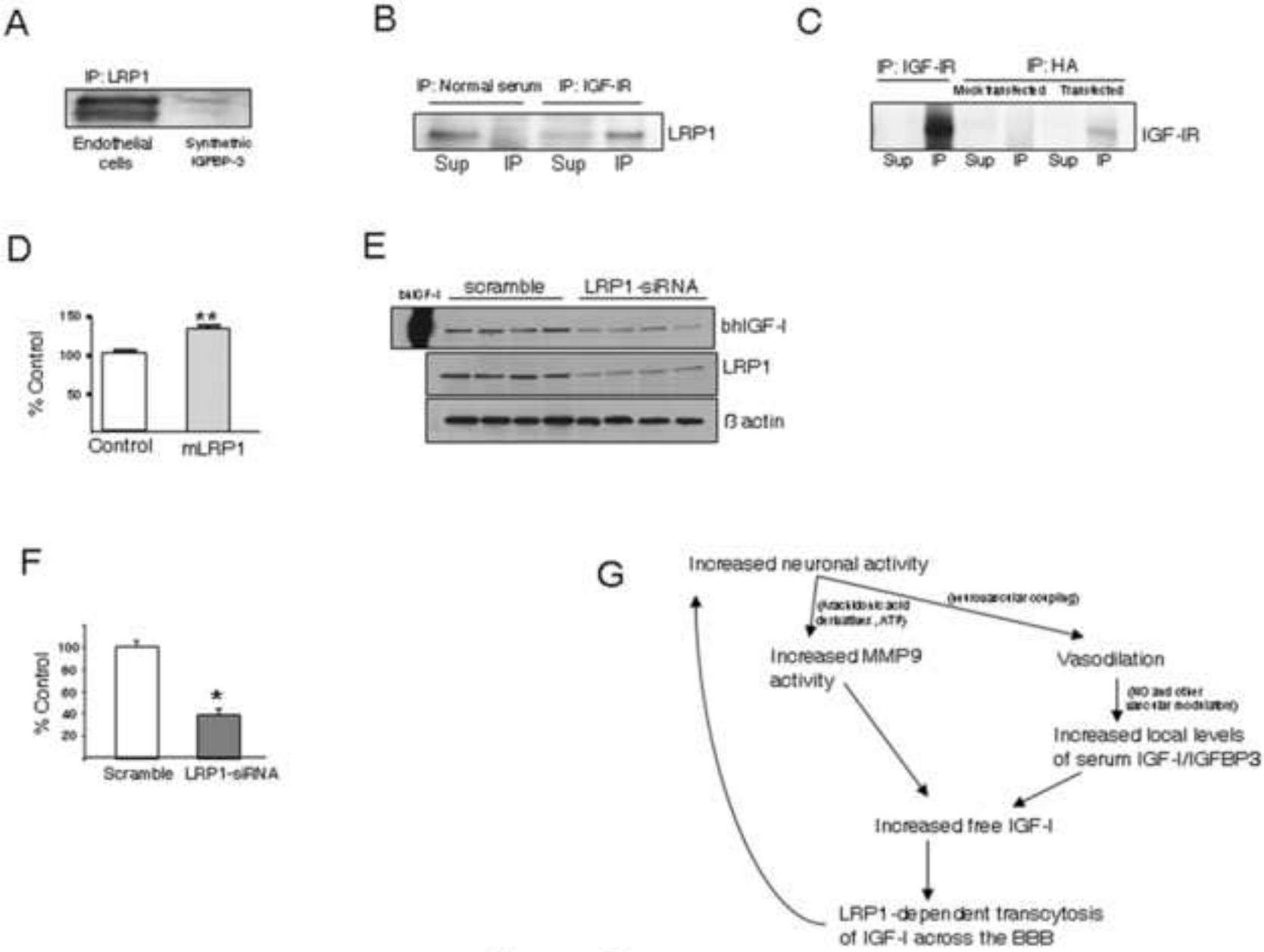

Figure 8

Inventory of supplemental information: Four figures. Figure S1 is related to Figure 1, Figure S2 is related to Figure 2, Figure S3 to Figure 4 and S4 to Figure 5. Supplementary experimental procedures are also included.

SUPPLEMENTARY DATA

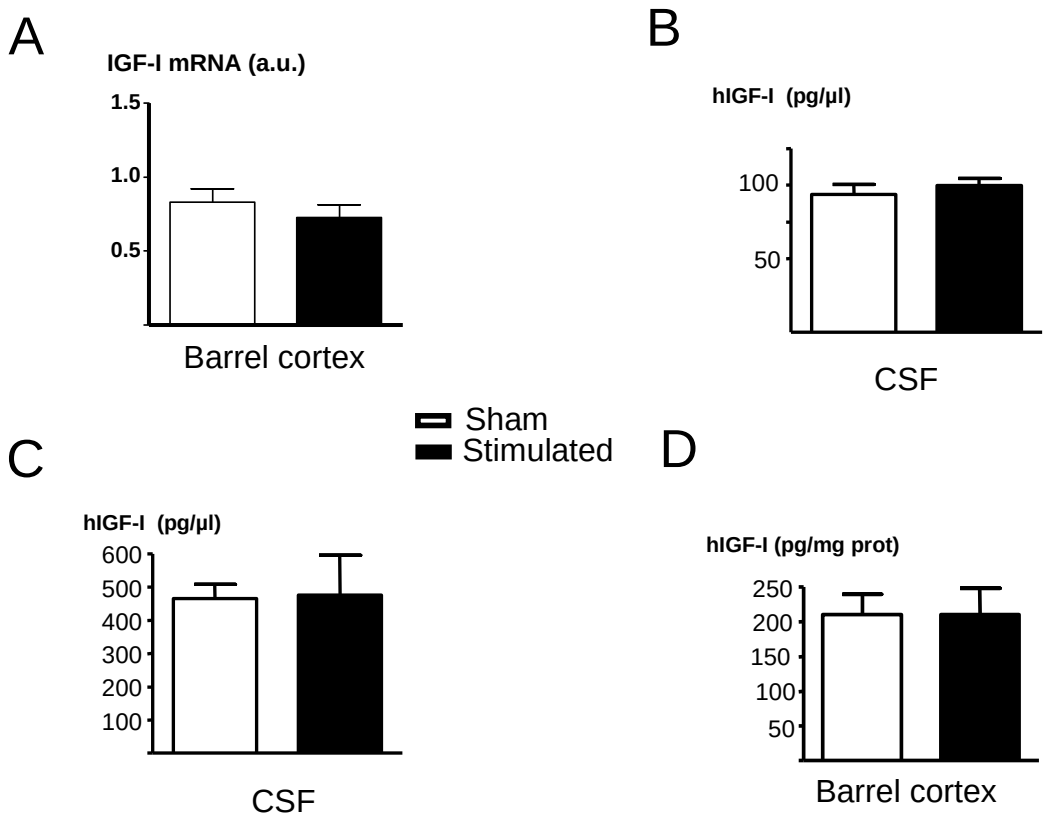

Supplementary Figure 1

Figure S1, related to Figure 1: **A**, Unilateral whisker pad stimulation did not alter IGF-I mRNA levels in the contralateral somatosensory cortex as determined by qPCR. Both the stimulated and unstimulated sides show similar IGF-I mRNA levels (n=6). **B,** Levels of hIGF-I in CSF were not altered by electrical stimulation of the whiskers (n=7). **C**, After icv administration of hIGF-I, its levels in CSF were similar in whisker-, and sham-stimulated rats (n=7). **D,** Levels of hIGF-I in somatosensory cortex of stimulated and non-stimulated rats previously injected icv with IGF-I. No differences were detected. (n=7).

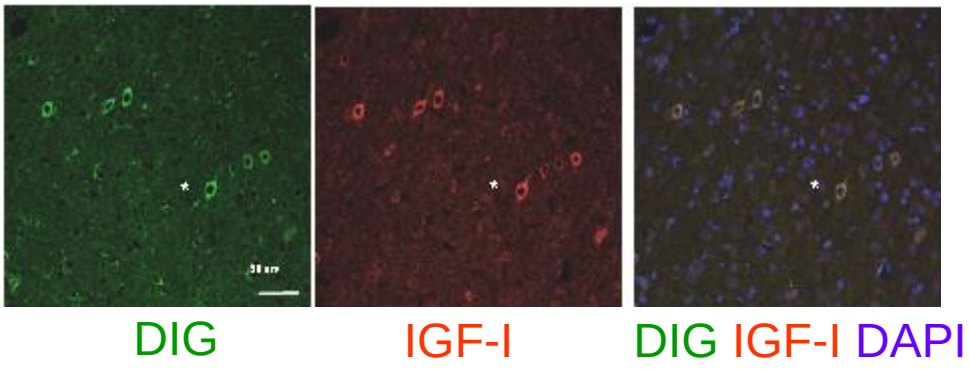

Supplementary Figure 2

Figure S2, related to Figure 2: Double immunostaining using anti-Dig and anti-IGF-I antibodies show that digoxigenin-stained cells in the barrel cortex of a vibrissae-stimulated rat contain IGF-I. DAPI staining marks cell nuclei.

A % change over baseline

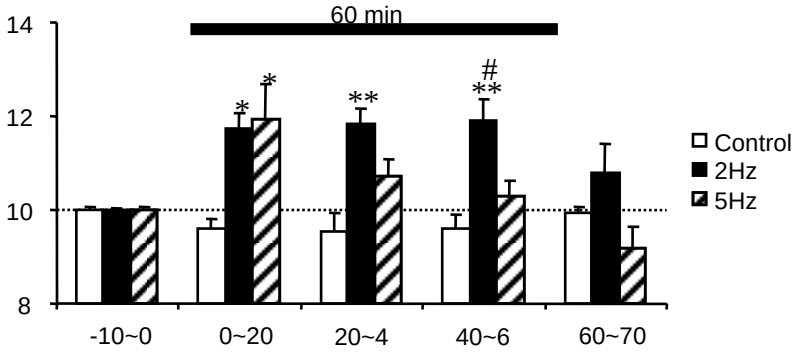

B % Changes in CBF

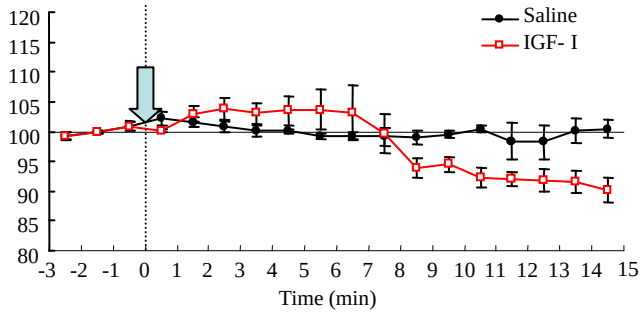

C % Increase in CBF

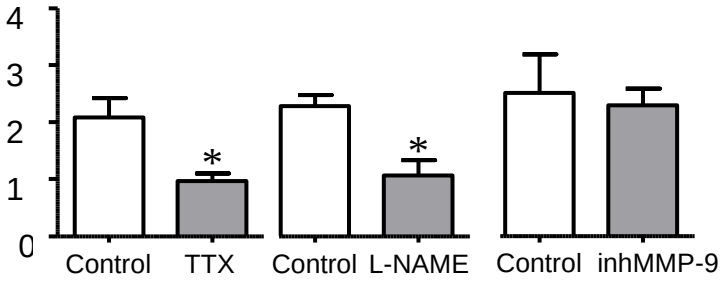

Supplementary Figure 3

Figure S3, related to Figure 4: **A**, Changes in cerebral blood flow (CBF) before and during vibrissae stimulation (60 min, solid line). While 2 Hz stimulation produced a consistent and significant increase in CBF, stimulation at 5 Hz produced a transient significant increase over the first 20 min. Data are averaged at 20 min intervals. * $p<0.05$, **$p<0.01$ vs. Control, # $p<0.05$ vs. 5Hz. **B,** Intracarotid injection of hIGF-I (50 μg/100 μl saline) did not alter CBF in the contralateral somatosensory cortex. IGF-I, n=3, saline, n=3. **C,** Infusion of either TTX (2 μM; n=5) or L-NAME (200 μM , n=5) into the barrel cortex markedly diminished the increase in CBF by 1 min of 2 Hz stimulation of the contralateral vibrissae. Infusion of an MMP9 inhibitor (10 μM, n=3) into the barrel cortex did not modify the CBF response to whisker pad stimulation (*$p<0.05$)

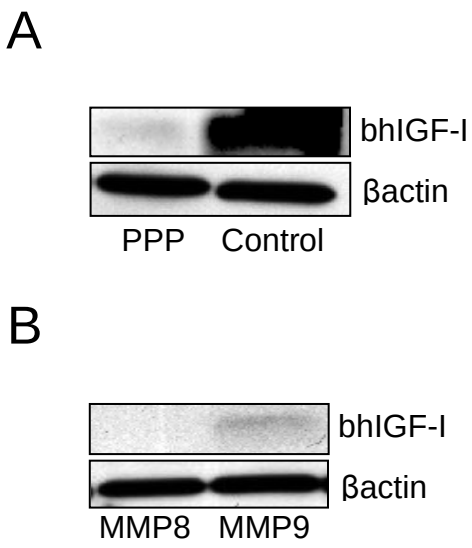

Supplementary Figure 4

Figure S4, related to Figure 5: **A,** Brain endothelial cells treated with the IGF-I receptor antagonist PPP internalized significantly less bhIGF-I than controls. (**p<0.01; n=3)**. B,** Treatment of endothelial cells with MMP8 did not increase bhIGF-I internalization by brain endothelial cells (n=3). Representative blots are shown.

Supplementary Experimental Procedures

Materials and animals. Male Wistar rats (225-350 g) and C57BL6J male mice (~30 grs; Harlan Labs; Barcelona, Spain) were used. Postnatal (4-7 days) rats were used for cell cultures. Animals were kept under standard diet and light/dark conditions following EU guidelines and handled according to institutionally-approved procedures. Human recombinant IGF-I was from ProSpec-Tany (Israel). Biotinylated IGF-I was from IBT (Germany). Digoxigenin-labelled IGF-I was produced following previously published procedures (Carro et al., 2000). The IGF-I receptor antagonist picropodophyllin (PPP) was from Sigma (USA). Primary antibodies used were: anti-digoxigenin (Roche, Switzerland, 1:500), anti panIGF-I (1:250, IBT), anti-βactin (1/100,000; Sigma), anti-$\beta_3$tubulin (1/2,000; Promega), anti-GFAP (1/2,000; Dako), and anti-LRP1 (Abcam, USA; recognizing a 37 KDa fragment of the protein), anti-IGF-IR (Sta. Cruz, USA), anti-pTyr (4G10 Platinum and PY20, Millipore, USA), and anti-MMP9 (Abcam), all used at 1:1000 dilution. Tomato lectin (1/500, Sigma) was used as a marker of brain endothelia. Secondary HRP-coupled streptavidin was from GE Healthcare (UK; 1:5000), secondary antibodies were from Bio-Rad (USA; 1/10,000), Alexa-coupled from Molecular Probes, (USA; 1/10,000) or biotinylated from Bio-Rad. The following compounds were also used: prostaglandin E_2 (PGE_2, 50 μM in vitro and 5 mM in vivo), 11,12 (Sigma) and 8,9 epoxyeicosatrienoic acid (EETs, 100 nM, Cayman Chem), ATP (10 nM), SNAP (an NO donor, 150 nM), L-NAME (a NO synthase inhibitor, 200 μM), tetrodotoxin (TTX, a sodium channel blocker, 2 μM), APMA (an activator of MMP9, 10 mM), MMP9 (50 ng/ml), MMP8 (50 ng/ml), MMP9 inhibitor (5 nM in vitro and 10 μM in vivo), IGFBP-3 (15 ng/ml), EGTA (10 mM), glutamate (100 μM), thapsigargin (ryanodine receptor inhibitor from Tocris, USA; 1 μM), Cox inhibitor Ibuprofen (Sigma, 200 μM), suramin (wide spectrum purinergic receptor

inhibitor, 100 µM), glutamate receptor inhibitors (Tocris; USA): AP5 (NMDA, 50 µM), CNQX (AMPA/Kainate, 20 µM), Ly367385 (mGluR type 1, 100 µM), MPEP (mGluR5, 50 µM), and PSA (IGFBP3 protease, 100 ng/ml).

In vivo procedures. hIGF-I was dissolved in saline and administered in the carotid artery through a cannula (20-50 µg/100µl saline) or into the brain lateral ventricle (20 µg/5 µl) following stereotaxic coordinates: AP: -1 mm from bregma; L: 1,2 mm from midline; DV: 4 mm from the surface. The IGF-I receptor antagonist PPP (2.5 µM) was dissolved in dimethyl sulfoxide whereas PGE_2 (5 mM) was dissolved in saline before intracortical injection. A microsyringe was lowered 0.5 mm into the primary somatosensory cortex. At the end of each experiment, animals were perfused thoroughly with saline. For immunocytochemical analysis brains were then handled as indicated below while for biochemical determinations brains were quickly removed, and frozen in dry ice; cerebellum and olfactory bulb were dissected before freezing the brain. For barrel cortex sampling, the remaining frozen brain was cut rostro-caudally using a cryotome in 0.5 mm slices until the medial fusion of the anterior commisure (-0.3 mm from bregma). Thereafter a 2 mm slice was made and a piece of the barrel cortex isolated through two incisions perpendicular to the surface of the cortex at 4.5 and 7 mm from midline. CSF was collected from the cisterna magna discarding those samples showing blood contamination.

Cerebral blood flow measurement. Rats were anesthetized with urethane (1.1 g/kg i.p.), and the anesthesia maintained with intermittent i.p. injections (~ 0.1 g/kg/h). The animals were stereotaxically fixed and a small craniotomy (5 x 5 mm) performed to expose the barrel cortex without removing the dura (coordinates: AP -1.5 ~ -2.0 mm; L 5.0 ~ 5.5 mm).

Cerebral blood flow (CBF) was continuously monitored using a laser-Doppler flowmeter (Omegawave, Japan) during whisker pad stimulation. The time constant was 0.01s. At the beginning of the recording the position of the Doppler probe was adjusted to monitor consistent and reproducible increases in CBF with brief whisker stimulations at 2Hz. After a 60 min stabilization period, the whisker pad was stimulated for 60 min at either 2 or 5 Hz. Control animals received sham electrical stimulation. Before and after whisker pad stimulation, arterial blood samples were collected and pH, PCO2, and PO2 immediately measured using an automated blood gas analyzer (Bayer, USA). Arterial blood pressure was continuously monitored and rectal temperature maintained at around 37°C using a heating pad (BRC, Japan). Flowmetry data were averaged at 5- or 20-min intervals and represented as relative changes versus baseline (recorded for an average of 10 min before stimulation).

In vivo recordings. A small hole was drilled in the skull over the SI cortex (50). Unit recordings in SI cortex (A 1-3 mm, L 2.5-4 mm from bregma) were recorded at 800 to 1500 μm below the brain surface using tungsten microelectrodes ; (2-5 MΩ; World Precision Instruments, Sarasota, USA). Unit firing was filtered (0.3-3 KHz), amplified (DAM80; World Precision Instruments) and fed into a PC computer (sample rate: 8 KHz) for off- line analysis with Spike 2 software (Cambridge Electronic Design, Cambridge, UK). Cortical field potentials were recorded at SI cortex, using tungsten macroelectrodes (1 MΩ). They were filtered (0.3 Hz-1 KHz), amplified and fed into the computer (sample rate: 3 KHz) Averages of the field potentials and summed peristimulus time histograms (PSTHs; 2 ms bins) were calculated from 20 stimuli. The mean tactile response was measured from

the PSTH as the number of spikes evoked at 10- 50 ms after stimulus onset and divided by the number of stimuli (n=20). The IGF-I receptor antagonist PPP (2.5 µM) was dissolved in dimethyl sulfoxide before intracortical injection and applied using a microsyringe lowered 0.5 mm into the primary somatosensory cortex. Data were compared using Student's paired t test and differences were considered statistically significant at the 95% level ($p<0.05$).

Immunoassays. hIGF-I was labeled with digoxigenin (Dig; Roche, Switzerland) and administered through the carotid artery (10 µg/100 gr). Animals were perfused transcardially with saline buffer and 4% paraformaldehyde in 0.1 M phosphate buffer, pH 7.4. Brain was serially sectioned at 40 µm. Immersed free-floating in 0.1 M phosphate buffer sections were assayed for Dig-IGF-I content using a anti-digoxigenin monoclonal antibody and/or rabbit anti panIGF-I, anti-GFAP, tomato lectin or anti-$\beta_3$tubulin. Secondary antibodies used were: biotinylated goat anti mouse (1:250, Pierce), alexa-488 conjugated donkey anti mouse and alexa-594 conjugated donkey anti rabbit (1: 1000, Molecular probes). Biotinylated antibodies were followed by the peroxidase-based ABC system (Pierce). In control experiments, first antibodies were omitted and no immunostaining was observed for any of the antibodies used (not shown).

A commercial hIGF-I ELISA (DSL or R&D Systems, USA) or an in-house rodent IGF-I ELISA were used to determine either hIGF-I or murine IGF-I. Lack of cross reactivity with rat IGF-I and human IGF-I, respectively was confirmed with rat IGF-I (IBT, Germany) or hIGF-I (not shown, but see(Trejo et al., 2007). Frozen brain samples were homogenized in 1 N acetic acid/4ºC, boiled for 20 min to eliminate the interference with IGF binding proteins, lyophilized and reconstituted in assay buffer. Boiled homogenate was centrifuged 1 min at 14,000 rpm and supernatant was frozen at -80 °C for 1 hour. Frozen protein extract

was lyophilized overnight and resuspended in PBS in the minimal volume necessary for analyzing IGF-I content in duplicate and total protein content in triplicate. When analyzing IGF-I levels in CSF, SEPAK cartridges were used to separate IGF-I from IGFBPs. Frozen dialysates were lyophilized and reconstituted with pretreatment buffer to eliminate IGF binding proteins interference.

A commercial ELISA (Cusabio CSB-E07967r) was used to measure PGE2 levels in cortical homogenates of sham-stimulated and vibrissae-stimulated rats following the manufacturer´s instructions.

Gel zymography. MMP-9 proteolytic activity was assessed by gelatin zymography. Endothelial/astrocyte co-cultures were treated with glutamate (100μM) or APMA (10mM) for 16h in serum-free conditions. Cells were washed three times with PBS and cell lysates collected and loaded under no reducing conditions onto gels (10% polyacrylamide , 1% gelatin). After electrophoresis, gels were washed twice in 2.5% Triton X-100 for 30 min to remove excess SDS and re-nature proteins. Gel were then incubated in developing buffer (50mM Tris-HCl, 200mM NaCl and 10mM $CaCl_2$) for 16h at 37ºC. To reveal the gelatinolytic activity, gels were stained with 0.25% brilliant blue for 30 min and then destained with 10% methanol and 7% acetic acid. Clear zones against the blue background indicate the presence of MMP9 proteolytic activity.

Pre-Embedding Immunogold Labeling and EM. Brains were perfused with 0.5% glutaraldehyde/2,5% paraformaldehyde and postfixed overnight. Vibratome sections (50 μm) were cut and blocked in PBS/5% BSA/5% NGS for 30 min, rinsed in incubation buffer

(1% BSA-C/PB), and incubated with antibody against digoxigenin (mouse 1:25; Roche Diagnostics GmbH) for 48 hr at 4°C. Sections were incubated with secondary antibody conjugated to colloidal gold (1:100 Electron Microscopy Sciences) during 24 hours at 4ºC and later enhanced with silver, washed, postfixed with 2.5% glutaraldehyde for 20 min, washed, and postfixed with 1% osmium tetroxide for 1 hr. Immunostained sections were dehydrated and embedded in Durcupan resin (Durcupan ACM; Fluka). Sixty nanometer sections were cut and collected on Formvar-coated single-slot grids, stained with uranyl acetate and lead citrate, and examined with a FEI Tecnai Spirit electron microscope.

Quantitative PCR. IGF-I qPCR was performed as described (Trejo et al., 2007). Briefly, after whisker pad stimulation (2 Hz, 1 hour), animals were perfused with cold saline. The brain was rapidly removed and the barrel cortices from both hemispheres dissected and snap frozen. Equivalent amounts of isolated total RNA served as template to synthesize cDNA using High Capacity cDNA Reverse Transcription Kit (Applied Biosystems, Foster City, CA) according to the manufacturer's instructions. TaqMan probes and primers for IGF-I and for the control housekeeping gene, rRNA 18s, were from the Assay-on-Demand gene expression products (Applied Biosystems). PCR was performed with the ABI PRISM 7500 Sequence Detection System (Applied Biosystems, Foster City, CA). The amount of IGF-I mRNA was normalized to the endogenous reference and expressed relative to the calibrator that was chosen randomly according to the comparative C_T method.